

Conjugate Additions of Cyclic Oxygen-Bound Nickel Enolates to α,β -Unsaturated Ketones

Celia M. Maya,^[a] Juan Cámpora,*^[a] Ernesto Carmona,*^[a] Inmaculada Matas,^[a] Pilar Palma,^[a] Enrique Gutiérrez-Puebla,^[b] and Angeles Monge^[b]

Dedicated to Professor Wolfgang Beck on occasion of his 75th birthday

Abstract: The reaction of nickel enolates displaying a metallacyclic structure with the α,β -unsaturated ketones methyl vinyl ketone (MVK) or methyl propenyl ketone (MPK) takes place in two stages, affording initially bicyclic adducts, which subsequently isomerize to the corresponding open-chain products. The former are generated with high stereoselectivity and can be considered as the products of the [2+4] cycloaddition of the enolate to the enone. The ring opening process involves a prototropic rearrangement that can be catalyzed by water. In the case of the

reaction of the parent nickel enolate complex **1** (which displays an unsubstituted Ni–O=C(R)CH₂ arrangement) with MVK, a double-addition process has been observed, consisting of two successive cycloaddition/isomerization reactions. The carbonylation of the different cyclic and noncyclic products affords the corresponding lactones that retain the stereochemistry of the or-

ganometallic precursors. This methodology allowed trapping the primary product of the reaction of **1** with MPK as the corresponding organic lactone, demonstrating that the cycloaddition process takes place with *exo* selectivity. DFT modeling of the latter reaction provides further support for a quasi-concerted cycloaddition mechanism, displaying a nonsymmetric transition state in which the C–C and the C–O bond are formed in an asynchronous manner.

Keywords: cycloaddition reactions • enolates • lactones • metallacycles • Michael addition • nickel

Introduction

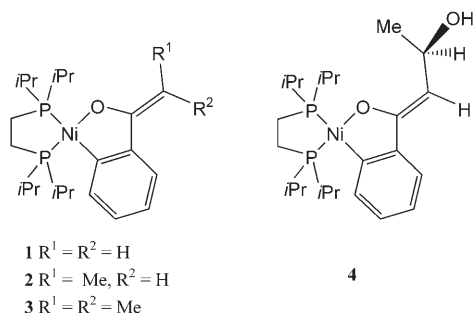
Metal enolates are an important class of reagents that find widespread use in many synthetic methods.^[1] Among these, late transition-metal enolates are finding important uses in a number of carbon–carbon bond-forming reactions,^[2] including many catalytic transformations, most of them involving

aldol-type additions^[3] and cross-coupling reactions.^[4] In recent years, they have also found use in catalytic Michael addition reactions,^[5] that is, enolate conjugate additions to α,β -unsaturated carbonyl compounds or other related functionalities.^[6] Although the reactivity of late transition-metal enolates has been thoroughly studied,^[7] very few examples of Michael additions of isolated complexes have been reported, in spite of the increasing importance of this reaction.^[8] The competitive acid–base exchange that may occur between the enolate and the acidic α,β -unsaturated ketone, to yield a mixture of enolate complexes, may represent a potential source of difficulties in this type of reactions.^[9]

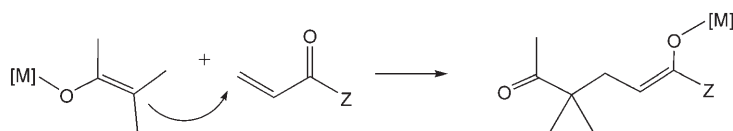
We have reported recently the synthesis and structural characteristics^[10] of metallacyclic, O-bound nickel enolates **1–3**, which are stabilized by the diphosphine *i*Pr₂PCH₂CH₂P*i*Pr₂ (dippe). The metallacyclic nature of these compounds disfavors the acid–base process and, therefore, converts them into suitable candidates for the above purpose. Indeed, compound **1** has been shown to react cleanly with an enolizable aldehyde^[10a,b] like MeC(O)H, to give the C–C coupling product **4**. In addition, we have re-

[a] Dr. C. M. Maya, Dr. J. Cámpora, Prof. E. Carmona, I. Matas, Dr. P. Palma
Instituto de Investigaciones Químicas
Departamento de Química Inorgánica
Consejo Superior de Investigaciones Científicas
Universidad de Sevilla, Centro de Investigaciones Científicas
“Isla de la Cartuja”, Avda. Américo Vespucio, s/n
Isla de la Cartuja, 41092 Sevilla (Spain)
Fax: (+34) 954-460-565
E-mail: campora@iiq.csic.es
carmona@us.es

[b] Prof. E. Gutiérrez-Puebla, Prof. A. Monge
Instituto de Ciencia de Materiales
Consejo Superior de Investigaciones Científicas
Campus de Cantoblanco, 28049 Madrid (Spain)



ported^[8a] that the cyclic structure of the enolate prevents the migration of the metal center between different oxygen atoms, as occurs in classic Michael additions (Scheme 1). This feature allows the isolation and characterization of unusual [2+4] cycloadduct intermediates, which subsequently evolve into open-chain addition products. Herein, we describe in full^[8a] the reactivity of nickel enolates **1–3** toward the α,β -unsaturated ketones methyl vinyl ketone (MVK) and *trans*-3-pente-2-one (abbreviated methyl propenyl ketone, MPK).

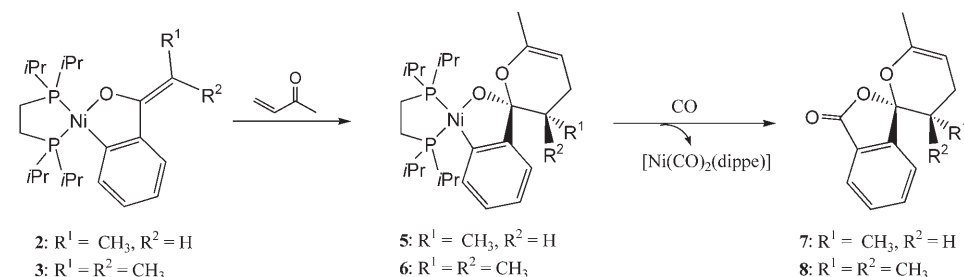


Scheme 1.

Results and Discussion

Reactions with methyl vinyl ketone: The cyclic enolates **1–3** react readily with MVK at room temperature, but while **2** and **3**, which contain a methyl-substituted enolate carbon, yield a single product, the reaction of the unsubstituted enolate **1** is more complex and gives rise to four products in a stepwise manner. Hence, for the sake of simplicity the reactivity of **2** and **3** will be considered first.

The two compounds **5** and **6** which are formed upon treatment of enolates **2** and **3**, respectively, with MVK at room temperature (Scheme 2), are moderately air-stable crystalline solids, which can be readily characterized by analytical and spectroscopic techniques (see Experimental Section). In



Scheme 2.

addition, most valuable structural information is provided in this case and in others later discussed by their carbonylation reactions, affording $[Ni(CO)_2(dippe)]$ along with the bicyclic lactones **7** and **8**, respectively. The NMR spectra of **5–8** are consistent with the represented spirocyclic structures, which can be taken as suggesting that the C–C bond-forming step leading to **5** and **6** involves a [2+4] addition of the enolate to the α,β -unsaturated ketone. Compound **5** is formed in a stereoselective manner, and only one diastereoisomer has been detected.^[11] The high selectivity strongly suggests a synchronous generation of the two stereogenic centers. Observation for **5** and **7** of NOE crosspeaks between the *CHMe* unique hydrogen atom and one of the aromatic resonances in the NOESY spectra of the two compounds indicates that the accompanying Me substituent and the phenylene unit maintain the relative *trans* configuration that is present in the starting enolate **2**.

Additional, unequivocal evidence for the stereochemistry of **5** and **6** has been provided by a single-crystal X-ray analysis of **5**.^[8a] As shown in Figure 1, this compound contains a spirocyclic organic fragment displaying an almost planar metallacyclic unit and a six-membered tetrahydropyran

ring. The latter displays a half-chair conformation, with the ONi and C_6H_4 substituents occupying axial and equatorial positions, respectively. As expected, the methyl substituent at C8 is *trans* to the aryl group. The nickel center has a distorted square-planar geometry,

characterized by Ni–O1 and Ni–C1 distances of 1.846(1) and 1.932(2) Å, respectively, and by Ni–P bonds which are somewhat different in lengths (Ni–P1 = 2.158(1); Ni–P2 = 2.207(1) Å). While the Ni–O1 bond length is comparable to that found in structurally characterized nickel enolate,^[10] hydroxo^[12] and alkoxo^[13] compounds, the C7–O1 bond is sufficiently short (1.365(2) Å), indicating some partial double-bond character, being, in fact, significantly shorter than the C7–O2 bond length of 1.469(2) Å. The latter distance is actually somewhat longer than that of a conventional single C–O bond (1.43 Å).^[14] These and other structural data justifies representation of the electronic structure of **5** (and by extension of **6** and related compounds) in terms of a resonance hybrid of canonical forms **I** and **II**. These are reminiscent of the hyperconjugative resonance description usually invoked to explain the so-called anomeric effect, observed in cyclic acetals and ethers, in which an electronegative substituent bound to the atom next to the oxygen atom tends to occupy the axial position, as happens with the ONi substituent of the tetrahydropyran ring of **5**.^[15] However,

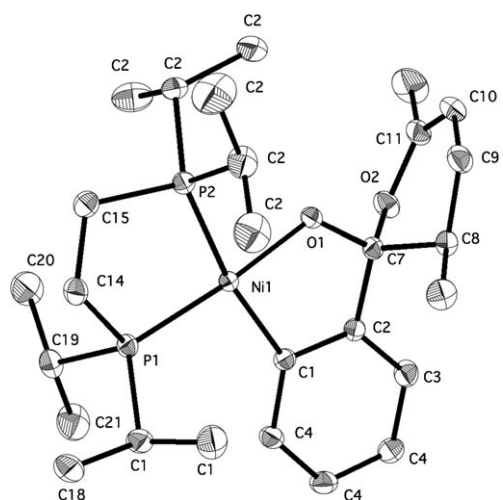
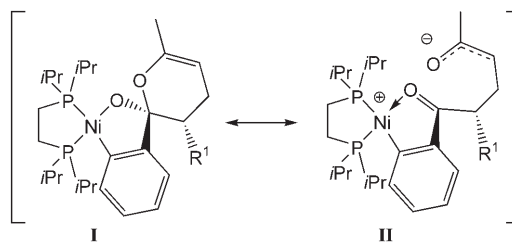


Figure 1. ORTEP drawing of **5**. Selected bond lengths (Å) and angles (°): Ni–O1 1.846(1), Ni–C1 1.932(2), Ni–P1 2.158(1), Ni–P2 2.207(1), O1–C7 1.365(2), O2–C7 1.469(2), O2–C11 1.377(2), C10–C11 1.317(3); O1–Ni–C1 86.16(7), O1–Ni–P2 84.84(5), P1–Ni–P2 88.56(3), C7–O1–Ni 117.7(1), O1–C7–O2 109.4(1).

the anomeric effect is probably not involved in determining the preferred configuration of the dihydropyran ring of **5**, as the bonding scheme depicted by **I** ↔ **II** (Scheme 3) involves the transfer of electron density from the lone pairs of the alkoxide fragment to the C–O(C) σ^* orbital. In turn, these are controlled by the relative orientations of the orbitals, which are imposed by the rigid and flat metallacyclic fragment and not by the 6-membered ring configuration.

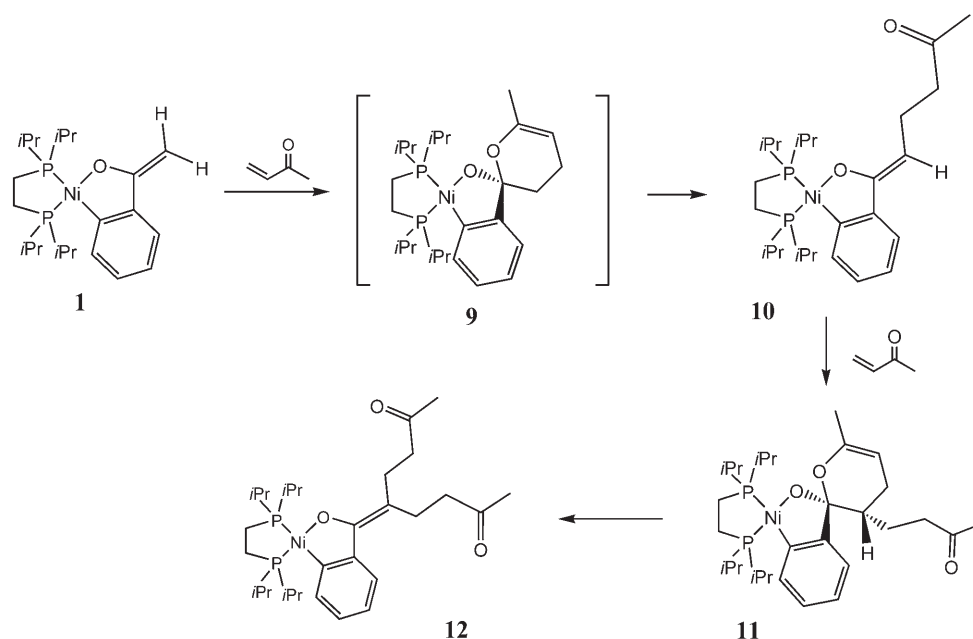
As mentioned at the beginning, the reaction of the unsubstituted enolate **1** with MVK is more complex and gives rise to four different products, **9–12**, with the structures repre-



Scheme 3.

sented in Scheme 4. Reacting **1** with stoichiometric amounts of MVK, at room temperature, for 1 h, by using THF as the reaction solvent yields a mixture of **9**, **10**, and **11**, in an approximate ratio of 6:1:2. If this reaction mixture is stirred for about 24 h at room temperature, compound **9** converts into **10**, while **11** remains unaltered. However, the use of two equivalents of MVK produces **9** and **11**, exclusively, although, once more, the former compound slowly disappears with time when the reaction mixture is further stirred at room temperature. As represented in Scheme 2, these observations may be explained by assuming that the stoichiometric reaction of **1** and MVK gives a mixture of **9** and **10**, with the former rearranging slowly into the latter, while in the presence of additional amounts of MVK, enolate **10** undergoes further reaction and converts into the bicyclic derivative **11**, which incorporates two molecules of the α,β -unsaturated ketone.

A bicyclic structure can also be proposed for **9** (see below) and therefore compounds **9** and **11** (and also **5** and **6**) are closely related from a structural point of view. Since, as represented in Scheme 2, **9** is proposed to rearrange to the open enolate structure **10**, compound **11** can be expected



Scheme 4.

to experience a similar rearrangement. Indeed, isolated samples of **11** convert slowly, over a period of 24 h, to an isomeric, open structure, characteristic of the disubstituted enolate **12**. On this basis, it could also be expected that compound **5** could undergo an isomerization of this kind, but we have not investigated this system any further. We have found that the ring-opening process is noticeably accelerated by the presence of added water, and this has allowed us to design improved experimental conditions for the isolation of complexes **10**, **11**, and **12**.

Characterization of the mixtures of products of this reaction is difficult, not only because of the diversity of the species, but also because of their lability, which has prevented isolation of some of them as analytically pure samples. Nonetheless, observation in the $^{31}\text{P}\{^1\text{H}\}$ NMR spectra of AX spin systems, with characteristic chemical shifts and coupling constants for each individual compound, considerably facilitates their identification and allows monitoring of their formation and subsequent rearrangement. In addition, the carbonylation of the nickelacycles is a highly selective reaction which gives the corresponding lactones in good yields. In this way, even if a mixture of lactones (and other carbonylation products, *vide infra*) is generated from the corresponding mixture of the open enolate, or the isomeric bicyclic structures (Scheme 5), their separation by standard chromatographic methods poses no problem. Structural identification of lactones **13–16** of Scheme 4 is unequivocal and straightforward; therefore, this reactivity provides a structur-

al probe for the nature of the organometallic precursors **9–12**.

Referring to the bicyclic compound **11** as a representative example, which may be prepared as an analytically pure microcrystalline solid, partial conversion into the isomeric species **12** (Scheme 2) occurs readily during the workup procedure, so that the isolated solid often contains about 4–5% of **12**. Notwithstanding, when this mixture is allowed to react with CO, the lactone **15** can be isolated as the main reaction organic product. NMR spectroscopic data presented in the Experimental Section are in accord with the proposed structure, which has been unequivocally confirmed by X-ray crystallography (Figure 2). As can be seen, the stereochem-

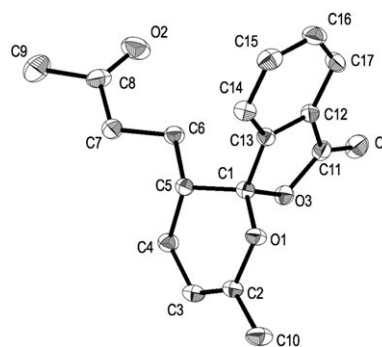
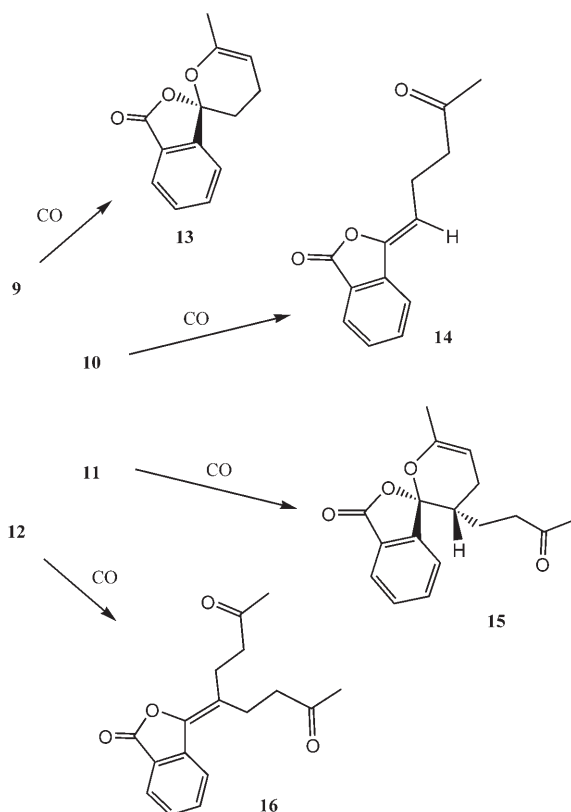


Figure 2. ORTEP view of compound **15**. Selected distances (Å) and angles (°): C11–O4 1.204(2), C11–O3 1.367(2), C1–O3 1.4680(14), C1–O1 1.4116(14), O1–C2 1.4054(14), C2–C3 1.319(2); O1–C1–O3 107.41(9).



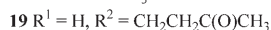
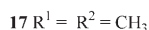
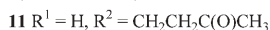
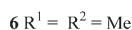
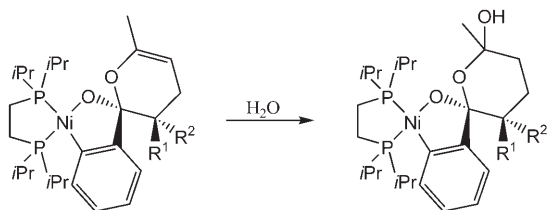
Scheme 5.

istry of the product is the same as that of **5**, with the $\text{CH}_2\text{CH}_2\text{CO}_2\text{R}$ group placed *trans* to the aromatic ring. As a whole, the formation of **11** from **1** and two molecules of MVC, represents a case of remarkable stereoselectivity, as the intermediate complex **10** is also formed exclusively with the *Z*-substitution pattern at the double bond. It is worth mentioning that the lactone **15** and the bicyclic compound **5** adopt the same conformation in the solid state, with the aryl group and the acetal oxygen atom occupying equatorial and axial positions, respectively (Figure 2). However, the alternation in the C–O distances discussed previously for **5**, does not exist for lactone **15**, and moreover, the relatively short C–ONi distance of 1.365(2) Å found in **5** is confronted by a corresponding C1–O3 distance of 1.4680(14) Å in **15**. This and other structural features of **5**, probably present in the analogous spirocyclic units of **9** and **11**, suggest a pronounced weakening of the dihydropyrane C–O bond by the strongly electron-donating alkoxide fragment, which is absent in the more stable dihydropyrane rings of the organic compounds.

The enolate compounds **10** and **12** have been isolated in a pure form and characterized by microanalysis and spectroscopy. Carbonylation of **10** affords lactone **14**, which exhibits a molecular ion with $m/z=216$ *uma* in the mass spectrum, indicating incorporation into the organic ligand of the enolate precursor **10** of only one molecule of MVK. In contrast,

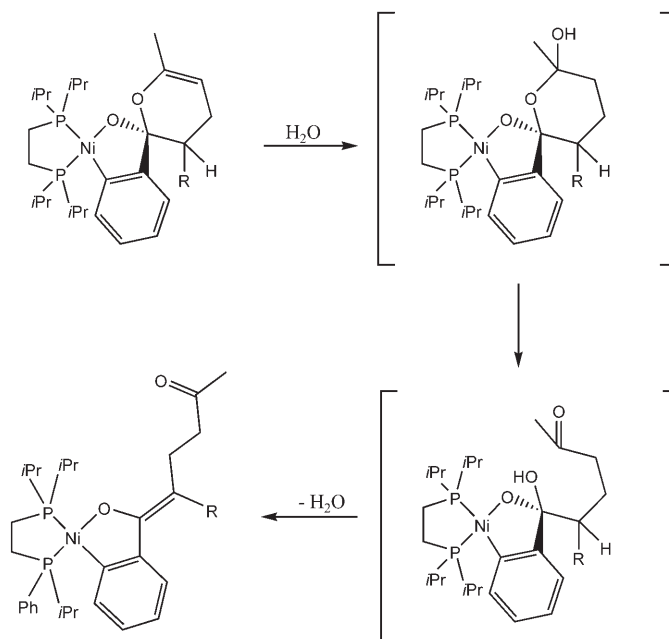
the molecular ions of **15** and **16** have $m/z = 286$ uma, revealing the presence of two molecules of MVK as part of the organic ligand of compounds **11** and **12**. Compound **9** is a very reactive intermediate which cannot be isolated in a pure form. However, optimization of the reaction time and reagents ratio allowed accumulation of a sufficient concentration of this species, which was subsequently carbonylated. From the resulting mixture of products, lactone **13** was isolated as the major organic component.

To gain information on the isomerization of the bicyclic compounds **9** and **11** to the enolates **10** and **12**, respectively, and to ascertain the role of added water in this process, we have studied the reaction of the latter substance with the bicyclic compound **6** described in this paper. As shown in Scheme 6, compound **6** adds a molecule of water across the



Scheme 6.

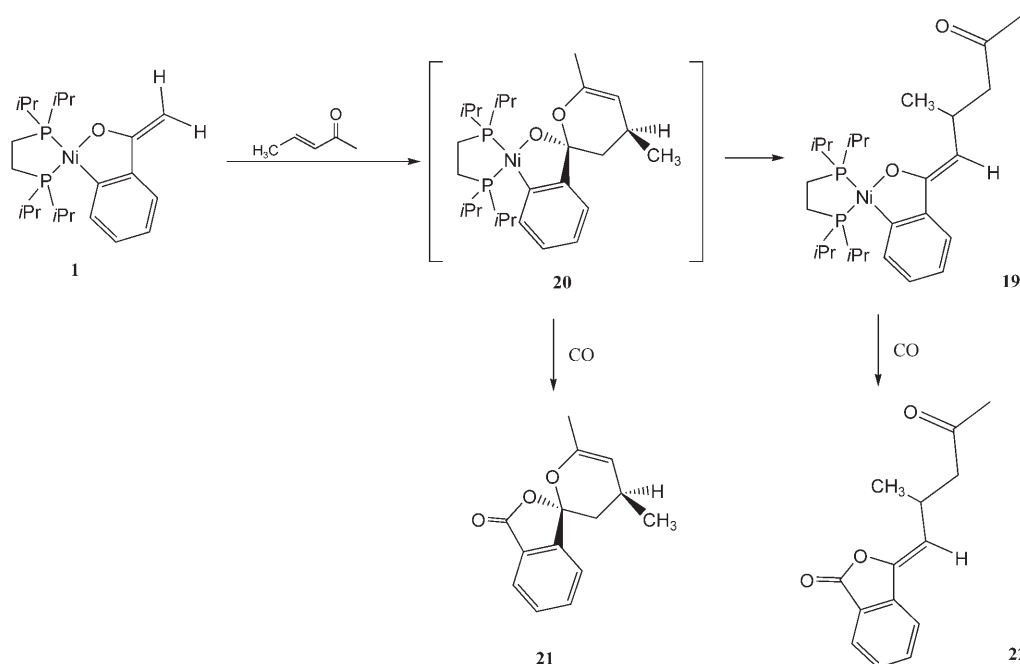
C=C bond to afford the hydrate **17**. The reaction is somewhat slow, but can be completed at 40 °C, in the presence of five equivalents of H₂O. The IR spectrum of **17** displays a broad absorption at approximately 3200 cm⁻¹ which reveals the presence of an OH functionality, also responsible for a low-field resonance (about $\delta = 8.7$ ppm) found in the ¹H NMR spectrum of **17**. In accord with the nature of this compound, its ¹H NMR spectrum shows no signals attributable to olefinic protons. The ³¹P{¹H} NMR spectrum of this compound is highly reminiscent of that of some transient species detected during the reaction of **1** with MVC in the presence of added water, suggesting that these could correspond to analogous hydrate derivatives. Indeed, the ³¹P{¹H} NMR spectrum of one such species matches that of a product, **18**, generated by reaction of a pure sample of compound **11** with water. Compound **18** proves too unstable to be isolated, as it readily evolves to the corresponding open Michael-like adduct **12** under the reaction conditions (Scheme 7). Notwithstanding this, careful analysis of the complex NMR spectra of the reaction mixture allowed full assignment of its ¹H and ¹³C resonances, confirming its identity. Thus, it seems likely that these hydrate complexes may be intermediates in the water-catalyzed ring-opening of the cycloadducts. The stability of **17** toward further rearrangement is probably due to the absence of eliminable hydrogen atoms on the six-membered ring. The observed reactivity of the C=C bond of **6** and **11** toward H₂O is not unexpected as



Scheme 7.

the analogous reaction of tetrahydropyran with water or alcohols is a well-known reaction, routinely used in synthesis as a protection method for the OH group.^[16]

Reactions with methyl propenyl ketone (MPK): To achieve a deeper understanding of the reactivity of nickel enolates with α,β -unsaturated ketones, we have studied the analogous reactions of methyl propenyl ketone. Somewhat surprisingly, the methyl-substituted enolates **2** and **3** do not react with MPK under ordinary conditions, while the unsubstituted compound **1** yields cleanly a single product **19** (Scheme 8). This has been formulated as a substituted enolate resulting from a C-C bond-forming reaction between the enolate carbon and the Me-substituted carbon atom of MPK. Characterization of **19** from the available data is straightforward (see Experimental Section), and monitoring its formation by ³¹P{¹H} NMR spectroscopy reveals the intermediacy of a product (**20** in Scheme 8) which proves to be too reactive to be isolated. As in similar instances already discussed, carbonylation of a reaction mixture enriched in **20** allows isolation of the spirocyclic lactone **21** from a mixture of products that contain also the isomeric, monocyclic lactone **22**, [Ni(CO)₂(dippe)], and the lactone resulting from the carbonylation of the unreacted parent enolate **1**.^[10b] Both **21** and **22** can be readily isolated from this reaction mixture, although **22** is best produced from isolated samples of **19** and CO. Comparison of their IR and NMR spectroscopic properties with those of related lactones (Schemes 1 and 4) demonstrates the close structural relationship which exists among these compounds. Once more, as the carbonylation reaction does not alter the structure of the organic chelating ligand within the metallacyclic unit of **20**, it can be assumed that this molecule is a [2+4] cycload-



Scheme 8.

duct analogous to **5**, **6**, **9**, and **11**, and that its formation precedes that of the open chain, Michael-type product **19**.

In close analogy with the related spirocyclic structures described in this work, compound **20** is formed as a single diastereomeric pair. The identity of the preferred diastereomer has been assigned on the basis of the 2D NOESY spectrum of the corresponding carbonylation product **21**. The assignment was helped with molecular models (DFT) of the two possible diastereomers, represented in Figure 3 together with a schematic representation of the spatial (NOE) relationships. The identity of the signals corresponding to H_a and H_s can be readily established on the basis of their coupling with H_m , which displays $^3J_{H,H}$ values of 12 and 6 Hz, consistent with approximately antiperiplanar and gauche dispositions, respectively. The observed product displays a distinct and selective NOE crosspeak between one of the *ortho* protons of the aromatic ring, H_{ar} , and H_s . This is consistent with diastereomer *RS,SR* (Figure 3a), while the other configuration (*RR,SS*; Figure 3b) should display the oppo-

site relationship (for example, $H_{ar}-H_a$). Additional cross-peaks linking H_m and H_s , as well as a nonspecific NOE interaction between the C5-Me and the two diastereotopic methylene protons provide additional support for the conformational assignment.

The high diastereoselectivity which characterizes the formation of the bicyclic organometallic products suggests that these are formed in a concerted manner, by means of an inverse electronic demand Diels–Alder mechanism.^[17] The fact that the formation of the cyclic adducts always precedes that of the open-chain products provides additional support for a cycloaddition mechanism. As shown in Scheme 9, the *syn* distribution of the Me and aryl groups in **20** (conformer a) in **21**) implies the *exo* approach of the MVK molecule to complex **1** with regard to the enolate oxygen atom. This is in contrast with most Diels–Alder reactions, which usually display the opposite selectivity due to favorable orbital interactions between the lone electron pairs of the heteroatom and the LUMO of the diene in the transition state (Alder's Rule). To identify the origin of the high stereoselectivity of the reaction of **1** with MVK, we have modeled this reaction by using DFT calculations.

To identify the origin of the high stereoselectivity of the reaction of **1** with MVK, we have modeled this reaction by using DFT calculations.

Theoretical modeling of the reaction of the nickel cyclic enolates with MPK: As we have shown previously,^[10b] the structure and reactivity of cyclic nickel enolates can be appropriately modeled with the DFT methods implemented in the

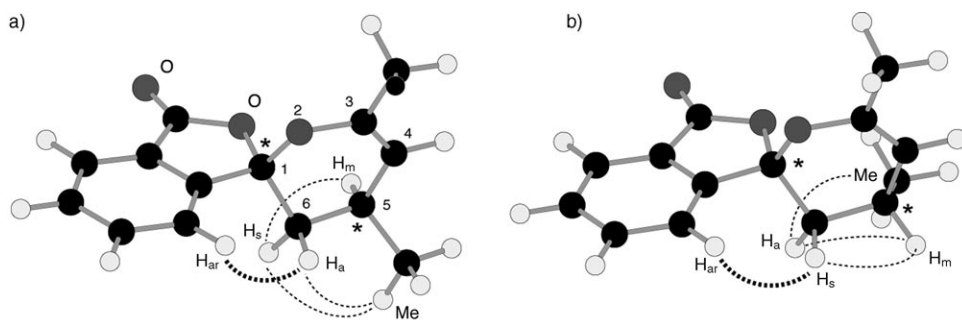
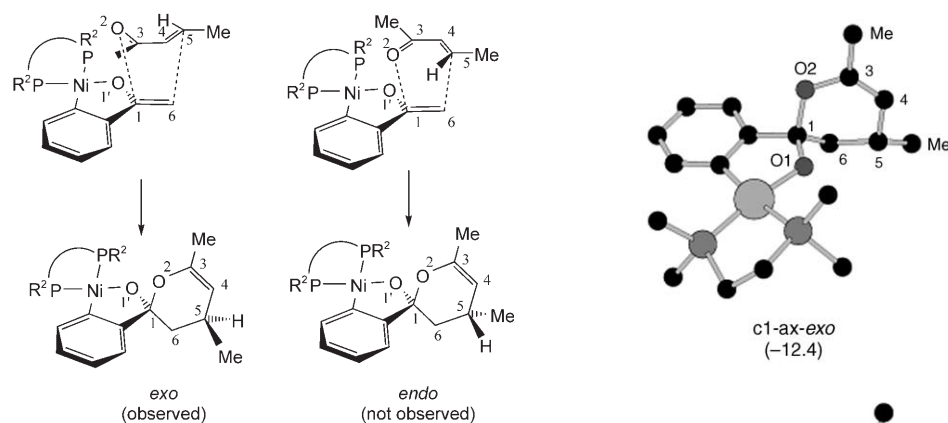


Figure 3. Molecular models for the two possible diastereoisomers of **21** (only one enantiomer represented), and relevant spatial (NOE) relationships. a) observed product (*SR,RS*); b) not observed (*SS,RR*).



Scheme 9.

Spartan Pro package, using the BP86 functional and the numerical basis set DN*. The calculations have been performed on molecules containing three different diphosphine ligands, displaying hydrogen (dpe), methyl (dmpe), or isopropyl (dippe) substituents at phosphorus. As in the previous paper, the preferred disposition of the isopropyl groups of the dippe ligand were previously determined by a molecular mechanics conformational analysis, fixing the positions of the core atoms of the organometallic complex, and then subjecting the five most stable conformers to full DFT optimization without imposed restrictions.

First, we will examine the structure and energetics of the organometallic cycloadducts. In contrast with the starting metallacyclic enolates, the organic moiety of these products is nonplanar, giving rise to two different conformations for the diphosphine ligand, which we have termed c1 and c2. In addition, the six-membered dihydropyran ring can adopt two possible half-chair conformations, with the ONi substituent occupying the axial (ax) or equatorial (eq) positions, respectively. Hence, considering the possible *exo* or *endo* stereochemical outcome of the addition reaction, eight possible product configurations have to be taken into account for each ligand. These are shown in Figure 4 for the dmpe ligand, together with their energies relative to the reagents (dmpe enolate + MPK). Table 1 collects some key bond lengths as well as the relative energies calculated for the products in their different configurations for the three diphosphine ligands.

It can be noted that, independently of the diphosphine ligand, the absolute energy minimum corresponds to the c1-ax-*exo* configuration, which is the same adopted by compound **5** in its solid-state structure. The geometric parameters calculated for these conformers are in good agreement (in general within 5%) with the experimental structure. The alternance of the C–O bond lengths of the acetal functionality is correctly reproduced by the calculations, which predict a short NiO1–C1 bond (1.39 Å) and a long C1–O2C bond (1.49 Å).

Not unexpectedly, the effect of the configuration of the diphosphine or the *exo*–*endo* isomerism on the modeled

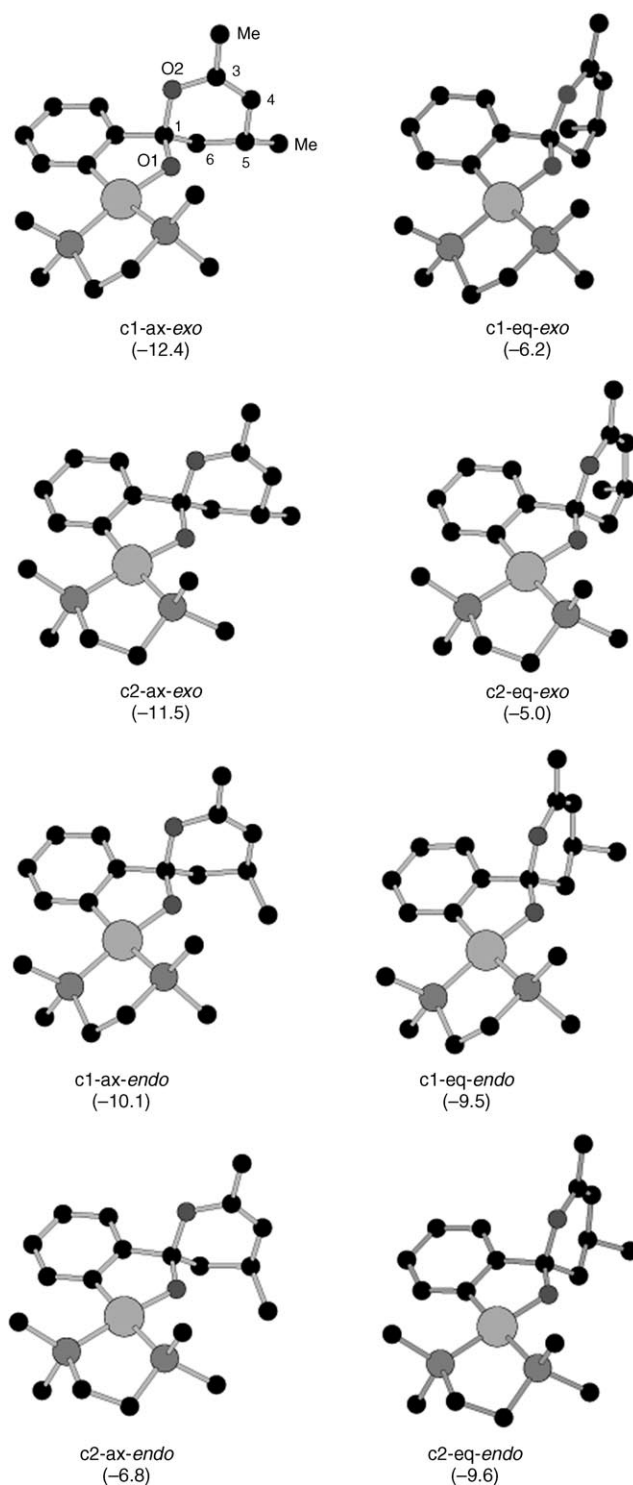


Figure 4. Eight possible configurations and relative energies (Kcal mol⁻¹) of the dmpe cycloaddition product.

bond lengths is very small (see Table 1). More noteworthy, these distances are neither affected by the axial or equatorial disposition of the ONi group. This can be taken in support by the lack of influence of the six-membered ring conformation on the pronounced bond length alternation characteristic of these molecules. Therefore, the stabilization of

Table 1. Key bond lengths^[a] and relative energies^[b] calculated for the bicyclic adducts of type **20** bearing the different diphosphine ligands.

Ligand	Anomer ^[c]	P–P conf. ^[d]	<i>exo</i>						Ni–O1	<i>E</i> ^[b]
			C1–C6	O1–C1	O2–C1	O2–C3	C3–C4			
dpe	ax	C1	1.54	1.40	1.47	1.38	1.36	1.85	–11.6	
	eq	C1	1.55	1.39	1.48	1.37	1.35	1.84	–4.5	
dmpe	ax	C1	1.55	1.39	1.49	1.37	1.35	1.87	–12.4	
	eq	C1	1.54	1.38	1.50	1.37	1.36	1.87	–6.2	
dippe	ax	C2	1.54	1.39	1.49	1.37	1.35	1.88	–12.6	

Ligand	Anomer ^[c]	P–P conf. ^[d]	<i>endo</i>						Ni–O1	<i>E</i> ^[b]	<i>E</i> _{exo} – <i>E</i> _{endo} ^[e]
			C1–C6	O1–C1	O2–C1	O2–C3	C3–C4				
dpe	ax	C1	1.54	1.40	1.48	1.37	1.35	1.83	–10.8	–0.3	
	eq	C1	1.55	1.40	1.47	1.37	1.35	1.85	–11.3		
dmpe	ax	C1	1.55	1.39	1.49	1.37	1.35	1.87	–10.1	–2.3	
	eq	C2	1.55	1.39	1.50	1.37	1.35	1.86	–9.6		
dippe	ax	C2	1.55	1.39	1.50	1.37	35	1.88	–7.2	–5.4	

[a] See Scheme 6 for numbering scheme. [b] Energies are relative to the corresponding enolate complex + MPK. [c] Relative to the axial (ax) or equatorial (eq) position of the ONi group. [d] Most stable conformation of the diphosphine ligand. [e] Energy difference between the most energetically favored isomers.

the *exo*-ax conformation is most likely due to steric causes rather than to the anomeric effect. Thus, it is readily noticed that the ax conformation is more stable for the *exo* configuration, but the difference is not so clear-cut for the *endo* isomers. A closer examination of the geometry of the *exo* derivatives reveals that the eq conformers display unfavorable axial–axial interactions between the aryl substituent and the C5-bound methyl group. Obviously, as the *exo* and *endo* configurations differ precisely in the disposition of the C5-Me group, the situation is the opposite for the latter, in which axial–axial interactions would occur between the mentioned C5-Me group and the O–Ni group in the ax conformation. However, as the steric encumbrance of the O–Ni entity is small, the energy difference between the ax and eq conformers in the *endo* configuration is small.

Analogously to the axial/equatorial preference, the preference for the *exo* versus the *endo* isomers can be explained on the basis of steric interactions. As already mentioned, the absolute energy minimum corresponds to the c1-ax-*exo* molecule, which is approximately 2 Kcalmol^{–1} more stable than the corresponding *endo* conformer (c1-ax-*endo*) in the dmpe models. A close look at the structures of these two isomers shows that the *endo* conformer is destabilized by an unfavorable interaction between a methyl group of the dmpe ligand and the C5-Me group, while the latter points away from the metal fragment in the *exo*. An interesting consequence of this observation is that the relative stability of the reaction products is controlled by the steric bulk of the ligand attached to the metal center. This conclusion is supported by the stability trends found for the unhindered dpe and the bulkier dippe ligands (Table 1).

We have limited the time-consuming calculation of the dippe derivatives to the more important ax conformers, but it can be seen that both series of molecules follow similar trends, allowing conclusions: 1) for the three ligands, the absolute energy minima correspond to the ax-*exo* configuration and 2) the thermochemical balance in favor of the *exo* product clearly increases with the ligand bulk, for example, dippe > dmpe > dpe. It is worth mentioning that the strict steric requirements of the dippe ligand shifts the preferred conformation of the dihosphine

ligand to c2. Another interesting point is that the reaction is somewhat less exothermic (by approximately 1 Kcalmol^{–1}) for dpe than for the tertiary phosphine ligands dmpe and dippe. The lower reactivity of the former can be traced out to the lower ligand basicity, which results in decreased nucleophilic character of the corresponding enolate. This is reflected in the lower energy of its HOMO, which is 6.5 and 7.4 eV below those of the dmpe and dippe enolates, respectively.

According to the precedent discussion, the stereoselectivity observed in the reaction of **1** with MPK is the same favored by the thermodynamic factors, for example, the relative stability of the possible products. However, the experimental observations suggest that the bicyclic organometallic products are probably formed through a cycloaddition mechanism, and this would imply a kinetic rather than thermodynamic control of the product stereochemistry. To check this possibility, we have searched for the transition states leading to such concerted cycloaddition with the three diphosphine ligands, to confirm whether such a mechanism is consistent with the observed stereoselectivity.

Table 2 collects the relative energies and some key bond lengths of the most stable conformers found for the transi-

Table 2. Key bond lengths^[a] and relative energies^[b] calculated for transition states corresponding to the addition of MPK to enolate molecules of type **1** containing different diphosphine ligands.

Ligand	P–P conf. ^[c]	<i>exo</i>						C5–C6	Ni–O1	<i>E</i> ^[b]
		C1–C6	O1–C1	O2–C1	O2–C3	C3–C4				
dpe	C1	1.40	1.33	3.21	1.25	1.44	2.06	1.89	14.0	
dmpe	C2	1.41	1.32	3.21	1.26	1.44	2.07	1.90	11.2	
dippe	C2	1.41	1.32	3.24	1.26	1.44	2.09	1.92	11.3	

Ligand	P–P conf. ^[c]	<i>endo</i>						Ni–O1	<i>E</i> ^[b]	<i>E</i> _{exo} – <i>E</i> _{endo} ^[d]
		C1–C6	O1–C1	O2–C1	O2–C3	C3–C4				
dpe	C2	1.41	1.32	3.17	1.25	1.44	2.03	1.89	14.1	–0.2
dmpe	C1	1.41	1.32	3.36	1.25	1.44	2.03	1.90	11.9	–0.7
dippe	C1	1.41	1.32	3.34	1.25	1.44	2.04	1.91	13.4	–2.1

[a] See Scheme 6 for numbering scheme. [b] Energies are relative to the corresponding enolate complex + MPK. [c] Most stable conformation of the diphosphine ligand. [d] Energy difference between the most energetically favored isomers.

tion states with the three diphosphines, and Figure 5 represents the *exo* and *endo* states, for the real dippe ligand. The geometry of the transition states is scarcely sensitive to the nature of the diphosphine or the *exo/endo* orientation of the

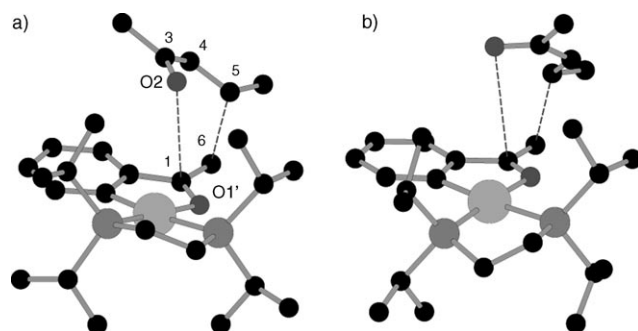


Figure 5. More stable conformations for the *exo* (a) and *endo* (b) transition states calculated for the reaction of the enolate **1** with MPK.

enone, and as can be seen in Table 2, all of them display close bond lengths and angles. Their general configuration, featuring almost planar enone and enolate fragments, indicate that the transition state is reached in an early stage of the addition process.

These transition states are far from expected for a perfectly concerted cycloaddition process. Thus, while there is an appreciable degree of bonding between the C5 and C6 atoms, the long C1...O2 distance (approximately 3.2 Å) indicates a very weak interaction. In spite of this, the relative disposition of the enone and enolate fragments favors the cancellation of the electric dipoles due to the negatively, O2, and positively C1 charged atoms, favoring the formation of the C–O bond. No intermediate stationary points could be found when the transition states are allowed to evolve to their corresponding cyclic products, and therefore the stereoselectivity of the process is much the same as if the two bonds were formed simultaneously. Obviously, the large separation between the carbonyl C3 and the enolate oxygen O1' prevents any significant orbital interactions at the *endo* transition states.

Both in the *exo* and *endo* configurations, the orientation of the enone fragment minimizes the steric repulsions by placing its C5-bound methyl group in an antiperiplanar position relative to C6. In such an arrangement, the orientation of the C5-Me group, which dictates the relative stability of the *exo* and *endo* bicyclic products, is nearly the same in the two transition states. As a consequence, the energy discrimination between the *endo* and *exo* approaching modes for the dpe or the dmpe ligands is very low (less than 1 Kcal mol⁻¹). However, as the size of the diphosphine ligand increases, the *endo* transition states become increasingly destabilized by the proximity of the C3-Me group of the MPK fragment, which, in contrast, remains relatively unhindered in the *exo* configuration. The destabilization becomes significant for the dippe system, and the energy difference between the two transition states (approximately, 2 Kcal mol⁻¹)

is sufficient to ensure more than 97% selectivity in favor of the *exo* selectivity, in good agreement with the experiment.

The coincidence of the kinetic and thermodynamic preferences of the addition reaction makes difficult to decide where the control step of the reaction stereoselectivity is. The energy difference in favor of the *exo* product (5.4 Kcal mol⁻¹) would lead to virtually complete selectivity under thermodynamic control conditions, while kinetic control could allow for a very small amount of the *endo* product, albeit in the limits of the experimental detection threshold. As shown by the bond stretch energy calculation, the C1–O2 bond is relatively weak, a mechanism for the thermodynamic control of the selectivity by reversible heterolytic dissociation of this bond cannot be ruled out. However, the experimental observation that the isomerization of the cyclic adducts to open-chain products is catalyzed by added water suggests that the ring-opening process may not be such a facile process under the reaction conditions.

Conclusion

Like other metal enolates, nickel enolates **1–3** react with α,β -unsaturated ketones to give addition products. However, their reactivity displays some interesting features which contrast with those observed in classic Michael reactions. Most important is the observation of bicyclic products, which later evolve into open-chain products. The structure of the former adducts and the high stereoselectivity that characterizes their formation strongly suggests that they are formed in a [2+4] cycloaddition process. DFT calculations indicate that such a process involves an early and nonsymmetric transition state, with the C–C bond formation taking place before the C and O atoms can actually interact, although the result would be indistinguishable from that of a truly concerted mechanism. Thus, the high degree of *exo* selectivity observed in the addition of **1** to MPK may be appropriately explained by the steric interactions of the bulky Ni-dippe fragment with the enone in such a transition state, but thermodynamic control of the stereochemistry cannot be fully excluded. In both experimental and calculated structures, the cyclic adducts display remarkably dissimilar C–O bond lengths in the acetal functionality. This feature evinces a weakening of the dihydropyran C–O bond by the strongly electron-donating alkoxy oxygen atom (O–Ni), and can be related to the tendency displayed by these complexes to undergo ring opening. Also in contrast with the usual Michael additions, the final products arise from a proton-transfer process (that can be catalyzed by water) and not from the migration of the metal center between oxygen atoms. This results in the regeneration of the enolate functionality in the final products. It is very likely that the ability of the metal center to jump between oxygen atoms is thwarted by the rigid metallacyclic structure, and in this sense it can be advanced that analogous [2+4] cycloadducts will be probably be observed in other conjugate addition reactions if the migration of the metal center is prevented. In the absence

of proton-transfer reactions, these cycloadducts may prove fairly stable. As we have shown in this work, these may find use in the synthesis of new organic molecules with a high level of stereoselectivity, expanding the already broad scope of applications of conjugated additions.

Experimental Section

All preparations and other operations were carried out under oxygen-free nitrogen by conventional Schlenk techniques. Solvents were rigorously dried and degassed before use. Microanalyses were performed by the Microanalytical Service of the Instituto de Investigaciones Químicas (Sevilla, Spain). Mass spectra of organic compounds (electronic impact) were measured at the General Research Service Center (CITIUS) of the University of Sevilla. IR spectra were recorded on a Bruker Vector 22 spectrometer, and NMR spectra on Bruker DRX 300, 400 and 500 MHz spectrometers. The ^1H and $^{13}\text{C}\{^1\text{H}\}$ NMR spectroscopic resonances of the solvent were used as the internal standard, but the chemical shifts are reported with respect to TMS, and $^{31}\text{P}\{^1\text{H}\}$ NMR spectroscopic shifts are referenced to external 85% H_3PO_4 . Where necessary, the spectral assignments have been helped with 2D COSY, HETCOR, and NOESY spectra. The nickel enolates **1–3** had been already prepared in our laboratory.^[10b] The b.p. of petroleum ether was 40–60°C.

[Ni(C₆H₄-o-C(CH₂(Me)CH₂CH=C(Me)O)O)(dippe)] (5): MVK (21 μL , 0.25 mmol) was added to a stirred suspension of complex **2** (117 mg, 0.25 mmol) in THF (5 mL) at -78°C . The mixture was stirred for 1 h at room temperature, after which time another half-equivalent (10.5 μL) of MVK was added. After 1 h, the reaction was shown to be complete by $^{31}\text{P}\{^1\text{H}\}$ NMR spectroscopy. The solvent was removed to obtain an orange oil which was washed twice with petroleum ether (20 mL). The complex was extracted with Et₂O (20 mL) and this solution was filtered. The volume was reduced and cooled to -30°C to provide 106 mg (81%) of yellow needles. ^1H NMR (C₆D₆, 20°C): δ = 0.77 (dd, 3H, $^3J_{\text{H,P}} = 11.7$, $^3J_{\text{H,H}} = 7.0$ Hz; CH₃), 0.79 (m, 2H; CH₂), 0.82 (dd, 3H, $^3J_{\text{H,P}} = 12.0$, $^3J_{\text{H,H}} = 7.0$ Hz; CH₃), 0.93 (dd, 3H, $^3J_{\text{H,P}} = 12.2$, $^3J_{\text{H,H}} = 7.1$ Hz; CH₃), 1.07 (m, 6H; CH₃), 1.12 (m, 2H; CH₂), 1.14 (d, 3H, $^3J_{\text{H,H}} = 6.3$ Hz; CH₃), 1.22 (dd, 3H, $^3J_{\text{H,P}} = 17.0$, $^3J_{\text{H,H}} = 7.3$ Hz; CH₃), 1.38 (dd, 3H, $^3J_{\text{H,P}} = 15.6$, $^3J_{\text{H,H}} = 7.2$ Hz; CH₃), 1.46 (dd, 3H, $^3J_{\text{H,P}} = 15.0$, $^3J_{\text{H,H}} = 7.1$ Hz; CH₃), 1.93 (m, 2H; CH), 1.98 (s, 3H; CH₃), 2.00 (m, 1H; CH), 2.15 (m, 2H; CHH, CH), 2.49 (m, 1H; CHH), 2.57 (m, 1H; CH), 4.75 (d, 1H, $^3J_{\text{H,H}} = 5.2$ Hz; =CH), 7.18 (m, 2H; CH_{ar}), 7.29 (m, 1H; CH_{ar}), 7.35 ppm (m, 1H; CH_{ar}); $^{31}\text{P}\{^1\text{H}\}$ NMR (C₆D₆, 20°C): AX spin system, $\delta_{\text{A}} = 73.7$, $\delta_{\text{X}} = 76.7$ ppm, $J_{\text{A,X}} = 23$ Hz; $^{13}\text{C}\{^1\text{H}\}$ NMR (C₆D₆, 20°C): δ = 16.1 (dd, $^1J_{\text{C,P}} = 19$, $^2J_{\text{C,P}} = 11$ Hz; CH₂), 17.8 (d, $^2J_{\text{C,P}} = 6$ Hz; CH₃), 17.9 (d, $^2J_{\text{C,P}} = 5$ Hz; CH₃), 18.4 (d, $^2J_{\text{C,P}} = 3$ Hz; CH₃), 18.6 (s; CH₃), 19.6 (d, $^2J_{\text{C,P}} = 5$ Hz; CH₃), 20.8 (d, $^2J_{\text{C,P}} = 6$ Hz; CH₃), 21.2 (d, $^2J_{\text{C,P}} = 6$ Hz; CH₃), 21.3 (s; CH₃), 22.6 (dd, $^1J_{\text{C,P}} = 25$, $^2J_{\text{C,P}} = 24$ Hz; CH₂), 23.2 (d, $^1J_{\text{C,P}} = 16$ Hz; CH), 24.5 (d, $^1J_{\text{C,P}} = 18$ Hz; CH), 25.1 (d, $^1J_{\text{C,P}} = 21$ Hz; 2 × CH), 28.3 (s; CH₂), 36.6 (s; CH), 93.8 (s; =CH), 117.3 (d, $^3J_{\text{C,P}} = 13$ Hz; O–C–O), 123.4 (s; CH_{ar}), 123.6 (s; CH_{ar}), 125.0 (d, $J_{\text{C,P}} = 7$ Hz; CH_{ar}), 137.2 (m; CH_{ar}), 150.1 (s; =C–O), 159.0 (dd, $^2J_{\text{C,P}} = 27$, 89 Hz; C_{ar}–Ni), 165.7 ppm (s; C_{ar}–C–O); IR (Nujol): $\tilde{\nu} = 1680$ cm⁻¹ (C=C); elemental analysis calcd for C₂₇H₄₆P₂O₂Ni: C 62.0, H 8.9; found: C 61.8, H 8.9.

[Ni(C₆H₄-o-C(CH₂(Me)CH₂CH=C(Me)O)O)(dippe)] (6): This compound was prepared as yellow needles in 83% yield by following the same procedure as for **5**. ^1H NMR (C₆D₆, 20°C): δ = 0.69 (m, 2H; CH₂), 0.74 (dd, 3H, $^3J_{\text{H,P}} = 11.0$, $^3J_{\text{H,H}} = 7.0$ Hz; CH₃), 0.84 (dd, 3H, $^3J_{\text{H,P}} = 10.6$, $^3J_{\text{H,H}} = 7.1$ Hz; CH₃), 0.88 (m, 2H; CH₂), 0.92 (dd, 3H, $^3J_{\text{H,P}} = 12.7$, $^3J_{\text{H,H}} = 7.0$ Hz; CH₃), 1.08 (m, 6H; CH₃), 1.24 (dd, 3H, $^3J_{\text{H,P}} = 16.6$ Hz, $^3J_{\text{H,H}} = 7.1$ Hz; CH₃), 1.33 (s, 3H; CH₃), 1.33 (dd, 3H, $^3J_{\text{H,P}} = 16.0$, $^3J_{\text{H,H}} = 7.5$ Hz; CH₃), 1.40 (dd, 3H, $^3J_{\text{H,P}} = 14.0$, $^3J_{\text{H,H}} = 7.0$ Hz; CH₃), 1.52 (s, 3H; CH₃), 1.68 (m, 1H; CH), 1.81 (m, 2H; CH, CHH), 1.97 (s, 3H; CH₃), 2.06 (m, 1H; CH), 2.37 (m, 1H; CH), 2.74 (m, 1H; CHH), 4.70 (d, 1H; $^3J_{\text{H,H}} = 3.5$ Hz; =CH), 7.13 (m, 2H; C_{ar}H), 7.26 (t, 1H, $^3J_{\text{H,H}} = 6.6$ Hz; C_{ar}H), 7.60 ppm (d, 1H, $^3J_{\text{H,H}} = 7.1$ Hz; C_{ar}H); $^{31}\text{P}\{^1\text{H}\}$ NMR (C₆D₆, 20°C): AX spin system, $\delta_{\text{A}} = 72.7$, $\delta_{\text{X}} = 75.9$ ppm, $J_{\text{A,X}} = 21$ Hz; $^{13}\text{C}\{^1\text{H}\}$ NMR (C₆D₆, 20°C): δ =

15.6 (dd, $^1J_{\text{C,P}} = 19$, $^2J_{\text{C,P}} = 11$ Hz; CH₂), 16.9 (d, $^2J_{\text{C,P}} = 6$ Hz; CH₃), 17.5 (d, $^2J_{\text{C,P}} = 6$ Hz; CH₃), 17.7 (d, $^2J_{\text{C,P}} = 2$ Hz; CH₃), 19.0 (s; CH₃), 19.5 (d, $^2J_{\text{C,P}} = 4$ Hz; CH₃), 20.2 (d, $^2J_{\text{C,P}} = 6$ Hz; CH₃), 20.8 (d, $^2J_{\text{C,P}} = 6$ Hz; CH₃), 21.0 (s; CH₃), 21.5 (d, $^2J_{\text{C,P}} = 6$ Hz; CH₃), 22.0 (d, $^1J_{\text{C,P}} = 15$ Hz; CH), 23.0 (dd, $^1J_{\text{C,P}} = 26$, $^2J_{\text{C,P}} = 23$ Hz; CH₂), 24.1 (d, $^1J_{\text{C,P}} = 19$ Hz; CH), 25.2 (d, $^1J_{\text{C,P}} = 18$ Hz; CH), 25.5 (s; CH₃), 26.0 (d, $^1J_{\text{C,P}} = 22$ Hz; CH), 27.2 (s; CH₃), 36.5 (s; C), 36.7 (s; CH₂), 93.7 (s; =CH), 118.4 (d, $^3J_{\text{C,P}} = 12$ Hz; O–C–O), 122.1 (s; C_{ar}H), 124.9 (d, $J_{\text{C,P}} = 7$ Hz; C_{ar}H), 125.6 (s; C_{ar}H), 137.0 (m; C_{ar}H), 148.9 (s; =C–O), 158.7 (dd, $^2J_{\text{C,P}} = 90$, 26 Hz; C_{ar}–Ni), 164.4 (s; C_{ar}–C–O); IR (Nujol): $\tilde{\nu} = 1675$ cm⁻¹ (C=C); elemental analysis calcd for C₂₈H₄₈P₂O₂Ni: C 62.6, H 9.0; found: C 62.2, H 8.8.

[Ni(C₆H₄-o-C(=CHCH₂CH₂C(O)Me)O)(dippe)] (10): Complex **1** (100 mg, 0.23 mmol) was dissolved in THF (20 mL) containing (4.1 μL , 0.23 mmol) of water. The mixture was cooled to -80°C and MVK was added (19 μL , 0.23 mmol). The solution was stirred at room temperature for 6 h. $^{31}\text{P}\{^1\text{H}\}$ NMR monitoring of the reaction mixture showed that it contained **10** as the major component, together with minor amounts of **1** and **11**. The solvent was stripped off under vacuum and the yellow residue was extracted with Et₂O and filtered. Partial evaporation of the solvent and cooling at -20°C led to the isolation of a crystalline sample of **10**, impurified by minor amounts of **1** (10%) and **14** (5%). Yield: 52%; ^1H NMR (C₆D₆, 20°C): δ = 0.73 (dd, 6H, $^3J_{\text{H,P}} = 11.6$, $^3J_{\text{H,H}} = 7.0$ Hz; CH₃), 0.77 (m, 2H; CH₂), 0.93 (dd, 6H, $^3J_{\text{H,P}} = 12.9$, $^3J_{\text{H,H}} = 7.1$ Hz; CH₃), 1.04 (m, 2H; CH₂), 1.11 (dd, 6H, $^3J_{\text{H,P}} = 17.1$, $^3J_{\text{H,H}} = 7.3$ Hz; CH₃), 1.38 (dd, 6H, $^3J_{\text{H,P}} = 15.5$, $^3J_{\text{H,H}} = 7.2$ Hz; CH₃), 1.86 (s, 3H; CH₃), 1.98 (m, 2H; CH), 2.12 (m, 2H; CH), 2.56 (t, 2H, $^3J_{\text{H,H}} = 7.7$ Hz; CH₂), 2.98 (td, 2H, $^3J_{\text{H,H}} = 7.7$, 7.2 Hz; CH₂–CH=), 5.11 (t, 1H, $^3J_{\text{H,H}} = 7.2$ Hz; =CH), 7.16 (m, 2H; C_{ar}H), 7.34 (t, 1H, $^3J_{\text{H,H}} = 5.8$ Hz; C_{ar}H), 7.69 ppm (d, 1H; $^3J_{\text{H,H}} = 5.3$ Hz; C_{ar}H); $^{31}\text{P}\{^1\text{H}\}$ NMR (C₆D₆, 20°C): AX spin system, $\delta_{\text{A}} = 73.3$, $\delta_{\text{X}} = 77.5$ ppm, $J_{\text{A,X}} = 22$ Hz; $^{13}\text{C}\{^1\text{H}\}$ NMR (C₆D₆, 20°C): δ = 16.1 (dd, $^1J_{\text{C,P}} = 20$, $^2J_{\text{C,P}} = 10$ Hz; CH₂), 18.1 (d, $^2J_{\text{C,P}} = 4$ Hz; CH₃), 18.2 (s; CH₃), 19.3 (d, $^2J_{\text{C,P}} = 4$ Hz; CH₃), 21.1 (d, $^2J_{\text{C,P}} = 6$ Hz; CH₃), 21.7 (s; CH₃), 22.4 (dd, $^1J_{\text{C,P}} = 26$, $^2J_{\text{C,P}} = 23$ Hz; CH₂), 23.9 (d, $^1J_{\text{C,P}} = 17$ Hz; CH), 25.2 (d, $^1J_{\text{C,P}} = 21$ Hz; CH), 29.3 (s; CH₃), 45.5 (s; CH₂), 90.5 (s; =CH), 121.4 (s; C_{ar}H), 123.3 (s; C_{ar}H), 124.3 (d, $J_{\text{C,P}} = 7$ Hz; C_{ar}H), 137.5 (m; C_{ar}H), 156.1 (s; C_{ar}–C–O), 158.2 (dd, $^2J_{\text{C,P}} = 88$, 26 Hz; C_{ar}–Ni), 169.9 (d, $^3J_{\text{C,P}} = 15$ Hz; C–O), 208.9 ppm (s, C=O); IR (Nujol): $\tilde{\nu} = 1710$ (C=O), 1610 cm⁻¹ (C=C).

[Ni(C₆H₄-o-C(CH₂(CH₂CH₂C(O)Me)CH₂CH=C(Me)O)O)(dippe)] (11): MVK was added (96 μL , 1.15 mmol) to a cooled (-80°C) solution of complex **1** (100 mg, 0.23 mmol) in THF (30 mL). The mixture was stirred at room temperature over 24 h, and then the solvent was evaporated under vacuum. The resulting residue was washed with petroleum ether, extracted with Et₂O and filtered. After partial concentration of the solution, cooling to -20°C furnished compound **11** as yellow crystals in 46% yield. The product was usually found to be impurified with small amounts of **12** (up to 5%), due to the unavoidable isomerization of **11** during the workup operations. Yield: 46%; ^1H NMR (C₆D₆, 20°C): δ = 0.77 (dd, 3H, $^3J_{\text{H,P}} = 11.5$, $^3J_{\text{H,H}} = 7.0$ Hz; CH₃), 0.80 (m, 2H; CH₂), 0.90 (m, 6H; CH₃), 1.06 (m, 6H; CH₃), 1.12 (m, 2H; CH₂), 1.25 (dd, 3H, $^3J_{\text{H,P}} = 16.9$, $^3J_{\text{H,H}} = 7.2$ Hz; CH₃), 1.41 (m, 6H; CH₃), 1.58 (s, 3H; CH₃–C=O), 1.77 (m, 2H; CHH), 1.88 (m, 3H; 2CH, CHH), 1.95 (s, 3H; CH₃), 2.01 (m, 1H; CH), 2.15 (m, 4H; 2CH, 2CHH), 2.34 (m, 1H; CHH), 4.71 (d, 1H, $^3J_{\text{H,H}} = 4.7$ Hz; CH), 7.14 (s, 2H; C_{ar}H), 7.27 ppm (s, 2H; C_{ar}H); $^{31}\text{P}\{^1\text{H}\}$ NMR (C₆D₆, 20°C): AX spin system, $\delta_{\text{A}} = 74.0$, $\delta_{\text{X}} = 76.8$ ppm, $J_{\text{A,X}} = 24$ Hz; $^{13}\text{C}\{^1\text{H}\}$ NMR (C₆D₆, 20°C): δ = 16.0 (dd, $^1J_{\text{C,P}} = 19$, $^2J_{\text{C,P}} = 11$ Hz; CH₂), 17.6 (s; CH₃), 17.8 (s; CH₃), 18.4 (s; CH₃), 18.5 (s; CH₃), 18.9 (s; CH₃), 19.7 (d, $^2J_{\text{C,P}} = 5$ Hz; CH₃), 20.9 (d, $^2J_{\text{C,P}} = 5$ Hz; CH₃), 21.2 (d, $^2J_{\text{C,P}} = 6$ Hz; CH₃), 21.3 (s; CH₃), 22.8 (m; CH₂, CH), 24.7 (d, $^1J_{\text{C,P}} = 19$ Hz; CH), 24.9 (d, $^1J_{\text{C,P}} = 21$ Hz; CH), 25.3 (d, $^1J_{\text{C,P}} = 21$ Hz; CH), 25.9 (s; CH₂CO), 27.1 (s; CH₂–CH₂CO), 28.7 (s; CH₃–C=O), 41.3 (s; CH–ring), 42.2 (s; CH₂–ring), 93.4 (s; =CH), 116.9 (d, $^3J_{\text{C,P}} = 12$ Hz; O–C–O), 123.3 (s; C_{ar}H), 123.7 (s; C_{ar}H), 125.2 (d, $J_{\text{C,P}} = 6$ Hz; C_{ar}H), 137.4 (s; C_{ar}H), 158.8 (dd, $^2J_{\text{C,P}} = 89$, 27 Hz; C_{ar}–Ni), 150.0 (s; O=C=), 165.7 (s; C_{ar}–C–O), 207.2 ppm (s; C=O); IR (Nujol): $\tilde{\nu} = 1710$ (C=O), 1670 cm⁻¹ (C=C); elemental analysis calcd for C₃₀H₅₀P₂O₂Ni: C 62.2, H 8.7; found: C 61.7, H 8.5.

[Ni(C₆H₄-o-C(=C(CH₂CH₂C(O)Me)₂O)(dippe)] (12): This compound was prepared according to the procedure described for **11**, but in this case the mixture was stirred at room temperature over 48 h. After this time, the solvent was removed, leaving an orange oil which was washed twice with petroleum ether. Extraction with Et₂O, filtration and concentration of the filtrate and cooling to -20°C for several hours provided yellow crystals of the complex. Yield: 58%; ¹H NMR (C₆D₆, 20°C): δ = 0.74 (dd, 6H, ³J_{HP} = 11.7, ³J_{HH} = 7.0 Hz; CH₃), 0.81 (m, 2H; CH₂), 0.96 (dd, 6H, ³J_{HP} = 12.6, ³J_{HH} = 7.0 Hz; CH₃), 1.03 (m, 2H; CH₂), 1.12 (dd, 6H, ³J_{HP} = 16.5, ³J_{HH} = 7.6 Hz; CH₃), 1.40 (dd, 6H, ³J_{HP} = 15.8, ³J_{HH} = 7.1 Hz; CH₃), 1.69 (s, 3H; CH₃CO), 1.90 (s, 3H; CH₃CO), 1.95 (m, 2H; CH), 2.20 (m, 2H; CH), 2.54 (t, 2H, ³J_{HH} = 7.8 Hz; CH₂-C=), 2.67 (t, 2H, ³J_{HH} = 8.1 Hz; CH₂-C=), 2.90 (t, 2H, ³J_{HH} = 8.1 Hz; CH₂CO), 3.00 (t, 2H, ³J_{HH} = 7.8 Hz; CH₂CO), 7.11 (t, 1H, ³J_{HH} = 7.5 Hz; C_{ar}H), 7.21 (t, 1H, ³J_{HH} = 7.5 Hz; C_{ar}H), 7.38 (t, 1H, ³J_{HH} ≈ ³J_{HP} = 6.8 Hz; C_{ar}H), 7.79 ppm (d, 1H, ³J_{HH} = 7.2 Hz; C_{ar}H); ³¹P{¹H} NMR (C₆D₆, 20°C): AX spin system, δ_A = 72.2, δ_X = 75.5 ppm, J_{AX} = 19 Hz; ¹³C{¹H} NMR (C₆D₆, 20°C): δ = 15.6 (m; CH₃), 18.1 (d, ²J_{CP} = 4 Hz; CH₃), 18.2 (s; CH₃), 19.5 (d, ²J_{CP} = 5 Hz; CH₃), 21.7 (d, ²J_{CP} = 6 Hz; CH₃), 22.6 (dd, ¹J_{CP} = 26, ²J_{CP} = 22 Hz; CH₂), 23.8 (d, ¹J_{CP} = 17 Hz; CH), 25.2 (d, ¹J_{CP} = 21 Hz; CH), 26.6 (s; CH₂CO), 28.7 (s; CH₂CO), 29.2 (s; CH₃CO), 43.6 (s; CH₂C=), 43.7 (s, CH₂C=), 104.5 (s; C=), 123.2 (s; C_{ar}H), 123.6 (s; C_{ar}H), 128.0 (s; C_{ar}H), 138.1 (s; C_{ar}H), 155.0 (d, ²J_{CP} = 2 Hz; C_{ar}-C=O), 160.4 (dd, ²J_{CP} = 87, 25 Hz; C_{ar}-Ni), 164.9 (s; C=O), 207.3 (s; C=O), 208.5 ppm (s; C=O); IR (Nujol) ν̄ 1705 (C=O), 1595 cm⁻¹ (C=C); elemental analysis calcd for C₃₀H₅₀P₂O₃Ni: C 62.2, H 8.7; found: C 61.7, H 8.5.

Synthesis of the bicyclic lactones C(O)(C₆H₄-o-C(C(R₁)(R₂)CH₂CH=C(Me)O)O (R¹, R²=H, Me, **7; Me, Me, **8**, and H, CH₂CH₂COMe, **15**):** These compounds were prepared by carbonylation of their corresponding organometallic precursors, as exemplified below for **7**. A stream of CO was bubbled for 5 min through a solution of compound **5** (100 mg, 0.17 mmol) in THF at room temperature. The resulting pale-yellow solution was evaporated to dryness and the oily residue was extracted with petroleum ether (30 mL) and filtered. The solution contains the organic product together with [Ni(CO)₂(dippe)], which were separated by spinning-band chromatography on a silica rotor, using a petroleum ether/diethyl ether 4:1 mixture.

Compound 7: Yield, 59%. ¹H NMR (C₆D₆, 20°C): δ = 0.41 (d, 3H, ³J_{HH} = 6.0 Hz; CH₃), 1.61 (d, 3H, ⁴J_{HH} = 0.8 Hz; CH₃), 1.81 (m, 1H; CHH), 2.06 (m, 2H; CHH, CH), 4.58 (d, 1H, ³J_{HH} = 5.0 Hz; =CH), 6.90 (t, 1H, ³J_{HH} = 6.8 Hz; CH_{ar}), 7.04 (m, 2H; CH_{ar}), 7.60 ppm (d, 1H, ³J_{HH} = 7.6 Hz; CH_{ar}); ¹³C{¹H} NMR (C₆D₆, 20°C): δ = 15.2 (s; CH₃), 19.2 (s; CH₃), 26.0 (s; CH₂), 32.7 (s; CH), 97.4 (s; =CH), 106.5 (s; O-C=O), 121.8 (s; CH_{ar}), 125.1 (s; CH_{ar}), 127.7 (s; C_{ar}-C=O), 130.2 (s; CH_{ar}), 133.8 (s; CH_{ar}), 147.2 (s; C_{ar}-C=O), 148.4 (s; =C=O), 167.6 ppm (s; C=O); HREIMS: m/z: calcd for C₁₄H₁₄O₃: 230.0943; found: 230.0940; IR (Nujol): ν̄ = 1775, 1685 cm⁻¹.

Compound 8: Prepared from **6** and purified by using a 1:1 mixture of petroleum ether/diethyl ether as eluant. Yield: 62%; ¹H NMR (C₆D₆, 20°C): δ = 0.57 (s, 3H; CH₃), 1.00 (s, 3H; CH₃), 1.49 (dd, 1H, ³J_{HH} = 16.7, ³J_{HP} = 5.4 Hz; CHH), 1.59 (s, 3H; CH₃), 2.34 (d, 1H, ²J_{HH} = 16.0 Hz; CHH), 4.53 (m, 1H; =CH), 6.89 (t, 1H, ³J_{HH} = 7.5 Hz; C_{ar}H), 7.00 (t, 1H, ³J_{HH} = 7.5 Hz; C_{ar}H), 7.13 (d, 1H, ³J_{HH} = 7.7 Hz; C_{ar}H), 7.62 ppm (d, 1H, ³J_{HH} = 7.6 Hz; C_{ar}H); ¹³C{¹H} NMR (C₆D₆, 20°C): δ = 18.9 (s; CH₃), 22.6 (s; CH₃), 23.2 (s; CH₃), 33.9 (s; CH₂), 34.2 (s; C-(CH₃)₂), 96.9 (s; =CH), 108.7 (s; O-C=O), 123.7 (s; C_{ar}H), 125.2 (s; C_{ar}H), 128.3 (s; C_{ar}-C=O), 130.1 (s; C_{ar}H), 133.2 (s; C_{ar}H), 146.2 (s; C_{ar}-C=O), 147.5 (s; =C=O), 167.4 ppm (s; C=O); IR (Nujol): ν̄ = 1780 (O-C=O), 1700 cm⁻¹ (C=C); HREIMS: m/z: calcd for C₁₅H₁₆O₃: 244.1099; found: 244.1101.

Compound 15: Prepared from **11** and purified by crystallization from CH₂Cl₂. Yield: 32%. ¹H NMR (C₆D₆, 20°C): δ = 1.19 (m, 2H; CHH), 1.79 (m, 3H; CH₃-C=O), 2.01 (s, 3H; CH₃), 2.06 (m, 1H; CHH), 2.26 (m, 2H; CHH), 2.36 (m, 2H; CHH, CH), 4.85 (d, 1H, ³J_{HH} = 5.5 Hz; =CH), 7.59 (d, 1H, ³J_{HH} = 7.6 Hz; C_{ar}H), 7.66 (t, 1H, ³J_{HH} = 7.5 Hz; C_{ar}H), 7.79 (t, 1H, ³J_{HH} = 7.5 Hz; C_{ar}H), 7.90 ppm (d, 1H, ³J_{HH} = 7.6 Hz; C_{ar}H); ¹³C{¹H} NMR (C₆D₆, 20°C): δ = 19.5 (s; CH₃-C=O), 23.7 (s; CH₂), 23.8 (s; CH₂), 29.9 (s; CH₃), 36.9 (s; CH), 40.3 (s; CH₂), 97.2 (s; =CH), 107.1 (s; O-C=O), 122.8 (s; C_{ar}H), 125.7 (s; C_{ar}H), 127.3 (s; C_{ar}-C=O), 131.2

(s; C_{ar}H), 135.1 (s; C_{ar}H), 147.4 (s; C_{ar}-C=O), 148.8 (s; =C=O), 168.5 (s; C=O), 207.6 ppm (s; CH₃-C=O); IR (Nujol): ν̄ = 1770, 1715, 1700 cm⁻¹ (C=O); HREIMS: m/z: calcd for C₁₅H₁₆O₃: 286.1205; found: 286.1203.

Preparation of the bicyclic lactone C(O)(C₆H₄-o-C(CH₂CH₂CH=C(Me)O)O (13): MVK (95 μL, 1.15 mmol) was added to a solution of complex **1** (100 mg, 0.23 mmol) in THF (25 mL) at -78°C. The mixture was stirred for 20 min at room temperature, after which time the major product was complex **9**, together with smaller amounts of the starting material and of complex **10**. At this moment CO was bubbled for 5 min, the solvent was evaporated under vacuum and the resulting residue was extracted with Et₂O (30 mL) and filtered. This solution contains a mixture of the compounds **13**, C(O)C₆H₄-o-C(=CHⁿ)O₂^[10b] **14**, and [Ni(CO)₂(dippe)], which were separated by spinning-band chromatography, using as eluent a 4:1 mixture of petroleum ether/Et₂O. Yield: 40%; ¹H NMR (C₆D₆, 20°C): δ = 1.43 (m, 1H; CHH), 1.60 (m, 3H; CH₃), 1.73 (m, 2H; CHH), 2.28 (m, 1H; CHH), 4.54 (d, 1H, ³J_{HH} = 4.8 Hz; =CH), 6.85 (m, 2H; C_{ar}H), 6.97 (d, 1H, ³J_{HH} = 3.8 Hz; C_{ar}H), 7.61 ppm (d, 1H, ³J_{HH} = 7.6 Hz; C_{ar}H); ¹³C{¹H} NMR (C₆D₆, 20°C): δ = 17.5 (s; CH₂), 19.4 (s; CH₃), 29.0 (s; CH₂), 96.9 (s; =CH), 103.6 (s; O-C=O), 121.9 (s; C_{ar}H), 125.3 (s; C_{ar}H), 128.2 (s; C_{ar}-C=O), 130.2 (s; C_{ar}H), 133.6 (s; C_{ar}H), 148.4 (s; C_{ar}-C=O), 148.8 (s; =C=O), 167.1 ppm (s; C=O); IR (Nujol): ν̄ = 1775 (O-C=O), 1685 cm⁻¹ (C=C); HREIMS: m/z: calcd for C₁₃H₁₂O₃: 216.0786; found: 216.0786.

Synthesis of the lactones C(O)(C₆H₄-o-C(=C(R¹)(R²)O (R¹, R²=H, CH₂CH₂COMe, **14 and R¹=R²=CH₂CH₂COMe, **16**):** The synthesis of these compounds was carried out by reaction of the corresponding organometallic complexes as described for **7**.

Compound 14: Prepared from **10**, and purified by using a 1:1 mixture of petroleum ether and diethyl ether. The product is the last to elute, after the nickel carbonyl and the lactones **13** and **15**. Yield: 55%; ¹H NMR (C₆D₆, 20°C): δ = 1.57 (s, 3H; CH₃), 1.99 (t, 2H, ³J_{HH} = 6.8 Hz; CH₂), 2.50 (q, 2H, ³J_{HH} = 7.1 Hz; CH₂), 5.33 (t, 1H, ³J_{HH} = 7.8 Hz; =CH), 6.77 (t, 1H, ³J_{HH} = 7.4 Hz; C_{ar}H), 6.85 (d, 1H, ³J_{HH} = 7.8 Hz; C_{ar}H), 6.90 (t, 1H, ³J_{HH} = 7.6 Hz; C_{ar}H), 7.55 ppm (d, 1H, ³J_{HH} = 7.7 Hz; C_{ar}H); ¹³C{¹H} NMR (C₆D₆, 20°C): δ = 20.0 (s; CH₃), 28.8 (s; CH₂), 41.9 (s; CH₂), 106.8 (s; =CH), 119.3 (s; C_{ar}H), 124.6 (s; C_{ar}-C=O), 124.9 (s; C_{ar}H), 129.0 (s; C_{ar}H), 133.4 (s; C_{ar}H), 139.2 (s; C_{ar}-C=O), 146.0 (s; C=O), 165.9 (s; O-C=O), 205.1 ppm (s; CH₃-C=O); IR (Nujol): ν̄ = 1775 (O-C=O), ν̄ = 1710 (C=O), 1605 cm⁻¹ (C=C); HREIMS: m/z: calcd for C₁₃H₁₂O₃: 216.0786; found: 216.0782.

Compound 16: Prepared from **12** and purified by using Et₂O as eluant. ¹H NMR (C₆D₆, 20°C): δ = 1.60 (s, 3H; CH₃), 1.62 (s, 3H; CH₃), 2.02 (t, 2H, ³J_{HH} = 8.0 Hz; CH₂), 2.16 (t, 2H, ³J_{HH} = 7.6 Hz; CH₂), 2.53 (t, 4H, ³J_{HH} = 7.7 Hz; CH₂), 6.79 (t, 1H, ³J_{HH} = 7.5 Hz; C_{ar}H), 6.99 (t, 1H, ³J_{HH} = 7.7 Hz; C_{ar}H), 7.48 (d, 1H, ³J_{HH} = 8.0 Hz; C_{ar}H), 7.68 ppm (d, 1H, ³J_{HH} = 7.7 Hz; C_{ar}H); ¹³C{¹H} NMR (C₆D₆, 20°C): δ = 24.7 (s; CH₂), 26.3 (s; CH₂), 29.4 (s; CH₃), 29.6 (s; CH₃), 41.3 (s; CH₂), 41.8 (s; CH₂), 122.9 (s; C_{ar}H), 125.1 (s; =C), 125.8 (s; C_{ar}H), 126.2 (s; C_{ar}-C=O), 129.0 (s; C_{ar}H), 134.4 (s; C_{ar}H), 138.4 (s; C_{ar}-C=O), 142.8 (s; =C=O), 166.1 (s; O-C=O), 205.7 (s; CH₃-C=O), 205.9 ppm (s; CH₃-C=O); IR (Nujol): ν̄ = 1765 (O-C=O), 1705 (C=O), 1610 cm⁻¹ (C=C); HREIMS: m/z: calcd for C₁₇H₁₈O₄: 286.1205; found: 286.1200.

Hydrate complexes C(O)(C₆H₄-o-C(C(R¹)(R²)CH₂CH₂C(OH)(Me)O)O (R¹=R²=Me, **17; R¹=H, R²=CH₂CH₂COMe, **18**):**

Compound 17: Water (73 μL, 3.5 mmol) was added to a solution of complex **6** (380 mg, 0.70 mmol) in THF (3.5 mL), and the resulting mixture was stirred for 5.5 h at 40°C. After this time, the solvent was evaporated under reduced pressure and the resulting solid was washed with 20 mL of petroleum ether, extracted with 30 mL of toluene, and filtered. Concentration of the solution, addition of some Et₂O, and cooling to -30°C provided yellow crystals. Yield: 46%; ¹H NMR (C₆D₆, 20°C) δ = 0.69 (m, 6H; CH₃), 0.80 (dd, 3H, ³J_{HP} = 12.1, ³J_{HH} = 7.0 Hz; CH₃), 0.87 (m, 2H; CH₂), 0.95 (dd, 3H, ³J_{HP} = 13.5, ³J_{HH} = 7.0 Hz; CH₃), 1.06 (dd, 3H, ³J_{HP} = 17.7, ³J_{HH} = 7.4 Hz; CH₃), 1.18 (m, 2H; CH₂), 1.22 (dd, 3H, ³J_{HP} = 17.3, ³J_{HH} = 7.2 Hz; CH₃), 1.40 (m, 7H; CHH, 2 × CH₃), 1.42 (s, 6H; CH₃), 1.78 (s, 3H; CH₃), 1.87 (m, 1H; CH), 1.95 (m, 1H; CH), 2.07 (m, 2H; CHH, CH), 2.19 (m, 1H; CH), 2.30 (td, 1H, ²J_{HH} = 13.4, ³J_{HH} = 4.5 Hz; CHH), 2.96 (td, 1H, ²J_{HH} = 13.2, ³J_{HH} = 4.2 Hz; CHH), 7.14 (m, 3H; C_{ar}H), 7.51

(m, 1H; C_{ar}H), 8.74 ppm (s, 1H; OH); ³¹P{¹H} NMR (C₆D₆, 20°C): AX spin system, δ_A=67.0, δ_X=75.7 ppm, J_{A,X}=19 Hz; ¹³C{¹H} NMR (C₆D₆, 20°C): δ=16.7 (dd, ¹J_{C,P}=21, ²J_{C,P}=10 Hz; CH₂), 17.9 (d, ²J_{C,P}=5 Hz; CH₃), 18.3 (d, ²J_{C,P}=6 Hz; CH₃), 18.6 (d, ²J_{C,P}=4 Hz; CH₃), 19.5 (s; CH₃), 19.7 (d, ²J_{C,P}=4 Hz; CH₃), 21.0 (d, ²J_{C,P}=7 Hz; CH₃), 21.4 (m; CH₃, CH₂), 22.7 (d, ²J_{C,P}=7 Hz; CH₃), 23.9 (d, ¹J_{C,P}=16 Hz; CH), 24.8 (d, ¹J_{C,P}=19 Hz; CH), 25.3 (s; CH₃), 25.3 (d, ¹J_{C,P}=14 Hz; CH), 26.5 (d, ¹J_{C,P}=24 Hz; CH), 29.0 (s; CH₃), 31.4 (s; CH₃), 32.5 (s; CH₂), 35.5 (s; CH₂), 37.7 (s; C), 99.0 (s; C–OH), 119.2 (d, ³J_{C,P}=13 Hz; O–C–O), 122.1 (s; C_{ar}H), 125.5 (s; C_{ar}H), 127.1 (s; C_{ar}H), 136.4 (dd, J_{C,P}=4, 8 Hz; C_{ar}H), 156.0 (dd, ²J_{C,P}=86, 29 Hz; C_{ar}–Ni), 163.9 ppm (s; C_{ar}–C–O); IR (Nujol): ν̄=3200 cm⁻¹ (OH); elemental analysis calcd for C₂₈H₃₀P₂O₂Ni: C 60.6, H 9.1; found: C 60.6, H 9.1.

Compound 18: This complex was formed when the bicyclic complex **18** was treated with water at room temperature in THF. It was characterized in solution, but it proved too unstable for isolation. ¹H NMR (C₆D₆, 20°C): δ=0.74 (m, 8H; CH₂, CH₃), 0.92 (m, 3H; CH₃), 1.07 (m, 8H; CH₂, CH₃), 1.32 (dd, 3H, ³J_{H,P}=17.6, ³J_{H,H}=7.0 Hz; CH₃), 1.44 (dd, 3H, ³J_{H,P}=14.4, ³J_{H,H}=7.0 Hz; CH₃), 1.51 (dd, 3H, ³J_{H,P}=17.3, ³J_{H,H}=7.0 Hz; CH₃), 1.56 (s, 3H; CH₃), 1.74 (s, 3H; CH₃–C=O), 1.80 (m, 1H; CH), 1.87 (m, 2H; CHH), 2.04 (m, 5H; CHH, CH), 2.17 (m, 2H; CHH), 2.30 (m, 1H; CH), 2.43 (m, 2H; CHH, CH), 7.18 (m, 2H; C_{ar}H), 7.35 (m, 2H; C_{ar}H), 8.59 ppm (s, 1H; OH); ³¹P{¹H} NMR (C₆D₆, 20°C): AX spin system, δ_A=68.5, δ_X=77.3 ppm, J_{A,X}=22 Hz; ¹³C{¹H} NMR (C₆D₆, 20°C): δ=16.3 (dd, ¹J_{C,P}=21, ²J_{C,P}=10 Hz; CH₂), 17.1 (d, ²J_{C,P}=6 Hz; CH₃), 18.0 (d, ²J_{C,P}=6 Hz; CH₃), 18.2 (d, ²J_{C,P}=5 Hz; CH₃), 19.0 (d, ²J_{C,P}=3 Hz; CH₃), 19.3 (s; CH₃), 20.7 (d, ²J_{C,P}=7 Hz; CH₃), 21.1 (t, J_{C,P}=23 Hz; CH₂), 21.6 (d, ²J_{C,P}=6 Hz; CH₃), 22.0 (d, ²J_{C,P}=6 Hz; CH₃), 22.9 (s; CH₂), 23.1 (d, ¹J_{C,P}=16 Hz; CH), 25.0 (d, ¹J_{C,P}=23 Hz; CH), 25.2 (d, ¹J_{C,P}=16 Hz; CH), 25.8 (d, ¹J_{C,P}=10 Hz; CH), 26.8 (s; CH₂), 28.9 (s; CH₃–C=O), 30.8 (s; CH₃), 38.8 (s; CH₂), 42.0 (s; CH₂), 45.5 (s; CH), 98.3 (s; C–OH), 117.7 (d, ³J_{C,P}=13 Hz; O–C–O), 123.7 (s; C_{ar}H), 124.3 (s; C_{ar}H), 125.4 (d, J_{C,P}=6 Hz; C_{ar}H), 136.4 (m; C_{ar}H), 155.7 (dd, ²J_{C,P}=86, 30 Hz; C_{ar}–Ni), 165.7 (s; C_{ar}–C–O), 207.0 (s; C=O).

[Ni(C₆H₄-o-C(=CHCH(CH₃)CH₂C(O)CH₃)O)(dippe)] (19): MPK (98 μL, 1 mmol) of was added to a solution of complex **1** (100 mg, 0.2 mmol) in THF (5 mL) at –78°C. The reaction mixture was stirred for 24 h at room temperature, after which time the solvent was evaporated under reduced pressure and the residue was extracted with Et₂O (20 mL). Concentration of the solution and cooling to –30°C provided 75 mg (72%) of yellow crystals. ¹H NMR (C₆D₆, 20°C): δ=0.73 (m, 6H; CH₃), 0.77 (m, 2H; CH₂), 0.93 (m, 6H; CH₃), 1.06 (m, 2H; CH₂), 1.10 (m, 6H; CH₃), 1.35 (d, 3H, ²J_{H,H}=7 Hz; CH₃–CH), 1.38 (m, 6H; CH₃), 1.95 (m, 2H; CH), 1.97 (s, 3H; CH₃–C=O), 2.06 (m, 1H; CH), 2.24 (m, 1H; CH), 2.43 (dd, 1H, ²J_{H,H}=14.6, ³J_{H,H}=7.9 Hz; CHH), 2.73 (dd, 1H, ²J_{H,H}=14.6, ³J_{H,H}=6.3 Hz; CHH), 3.87 (m, 1H; CH₂–CH), 4.92 (d, 1H, ³J_{H,H}=8.1 Hz; =CH), 7.16 (m, 2H; CH_{ar}), 7.33 (m, 1H; CH_{ar}), 7.65 ppm (m, 1H; CH_{ar}); ³¹P{¹H} NMR (C₆D₆, 20°C): AX spin system, δ_A=73.7, δ_X=77.4 ppm, J_{A,X}=22 Hz; ¹³C{¹H} NMR (C₆D₆, 20°C): δ=16.5 (dd, ¹J_{C,P}=20, ²J_{C,P}=10 Hz; CH₂), 18.4 (s; CH₃), 18.4 (d, ²J_{C,P}=5 Hz; CH₃), 18.7 (d, ²J_{C,P}=4 Hz; CH₃), 18.9 (s; CH₃), 19.5 (d, ²J_{C,P}=4 Hz; CH₃), 20.0 (d, ²J_{C,P}=5 Hz; CH₃), 21.5 (d, ²J_{C,P}=5 Hz; CH₃), 21.6 (d, ²J_{C,P}=5 Hz; CH₃), 22.9 (s; CH₃–CH), 23.0 (dd, ¹J_{C,P}=26, ²J_{C,P}=23 Hz; CH₂), 24.0 (d, ¹J_{C,P}=17 Hz; CH), 24.7 (d, ¹J_{C,P}=17 Hz; CH), 25.6 (d, ¹J_{C,P}=22 Hz; CH), 25.8 (d, ¹J_{C,P}=22 Hz; CH), 28.1 (s; CH₃–CH), 30.5 (s; CH₃–C=O), 53.2 (s; CH₂), 98.2 (s; =CH), 121.8 (s; CH_{ar}), 123.6 (s; CH_{ar}), 124.7 (d, J_{C,P}=7 Hz; CH_{ar}), 138.1 (m; CH_{ar}), 156.6 (s; C_{ar}–C–O), 158.9 (dd, ²J_{C,P}=27, 87 Hz; C_{ar}–Ni), 208.4 (s; C=O); IR (Nujol): ν̄=1710 (C=O), 1605 cm⁻¹ (C=C); elemental analysis calcd for C₂₇H₄₆P₂O₂Ni: C 62.0, H 8.9; found: C 61.6, H 8.9.

Synthesis of the bicyclic lactone C(O)(C₆H₄-p-C(CH₂CH(CH₃)CH=C(CH₃)O)O (21): A mixture of complex **1** (100 mg, 0.2 mmol) and MPK was stirred for 45 min at room temperature. ³¹P{¹H} NMR showed that **5** was the major species. Through this solution, a stream of CO was bubbled for 5 min at room temperature and the solvent was removed under vacuum. The residue was extracted with 30 mL of petroleum ether, the resulting solution was taken to dryness and the residue underwent spinning-band chromatography. Elution with 3:2 petroleum ether/Et₂O gave

compound **7** (24 mg, 53%) as a white solid. ¹H NMR (C₆D₆, 20°C): δ=0.81 (d, 3H, ³J_{H,H}=7.0 Hz; CH₃–CH), 1.39 (dd, 1H, ²J_{H,H}=13.4, ³J_{H,H}=6.0 Hz; CH₂H), 1.46 (dd, 1H, ²J_{H,H}=13.2, ³J_{H,H}=12.0 Hz; CHH_a), 1.61 (m, 3H; CH₃–C=), 2.57 (m, 1H; CH_m), 4.45 (m, 1H; =CH), 6.86 (t, 1H, ³J_{H,H}=7.3 Hz; CH_{ar}), 6.98 (m, 2H; CH_{ar}), 7.63 ppm (d, 1H, ³J_{H,H}=7.3 Hz; CH_{ar}); ¹³C{¹H} NMR (C₆D₆, 20°C): δ=19.2 (s; CH₃–C=), 20.5 (s; CH₃–CH), 23.6 (s; CH_m), 37.8 (s; CH_sH_a), 104.0 (s; =CH), 104.2 (s; O–C–O), 121.9 (s; CH_{ar}), 125.2 (s; CH_{ar}), 127.0 (s; C_{ar}–C=O), 130.3 (s; CH_{ar}), 133.6 (s; CH_{ar}), 147.9 (s; C_{ar}–C–O), 148.3 (s; =C–O), 167.2 ppm (s; O–C=O); IR (Nujol): ν̄=1775 (C=O), 1685 cm⁻¹ (C=C); HREIMS: m/z: calcd for C₁₄H₁₄O₃: 230.0943; found: 230.0940.

Synthesis of the lactone C(O)(C₆H₄-o-C(=CH(CHMeCH₂COMe))O (22): This compound was prepared in 53% yield from complex **19** following the same procedure described for **7**, and purified by spinning-band chromatography using a 2:3 mixture of petroleum ether and Et₂O as eluent. ¹H NMR (C₆D₆, 20°C): δ=1.00 (d, 3H; ³J_{H,H}=6.9 Hz; CH₃), 1.65 (s, 3H; CH₃–C=O), 2.04 (dd, 1H, ²J_{H,H}=16.3, ³J_{H,H}=6.6 Hz; CHH), 2.16 (dd, 1H, ²J_{H,H}=16.3, ³J_{H,H}=6.8 Hz; CHH), 3.27 (m, 1H; CH), 5.23 (d, 1H, ³J_{H,H}=9.2 Hz; =CH), 6.78 (t, 1H, ³J_{H,H}=7.1 Hz; C_{ar}H), 6.91 (m, 2H; C_{ar}H), 7.54 ppm (d, 1H, ³J_{H,H}=7.7 Hz; C_{ar}H); ¹³C{¹H} NMR (C₆D₆, 20°C): δ=20.0 (s; CH₃), 27.3 (s; CH), 29.1 (s; CH₃–C=O), 49.6 (s; CH₂), 112.1 (s; =CH), 119.4 (s; C_{ar}H), 124.5 (s; C_{ar}–C=O), 125.0 (s; C_{ar}H), 129.1 (s; C_{ar}H), 133.5 (s; C_{ar}H), 139.3 (s; C_{ar}–C–O), 144.8 (s; =C–O), 165.9 (s; O–C=O), 205.0 ppm (s; CH₃–C=O); IR (Nujol): ν̄=1610 (C=C), 1780 (O–C=O), 1715 cm⁻¹ (C=O); HREIMS: m/z: calcd for C₁₄H₁₄O₃: 230.0943; found: 230.0941.

Computational details: All calculations were performed by using the package Spartan Pro.^[18] Initial guess of the molecular geometry was obtained with the semiempirical PM3 method, and the resulting structures were fully optimized without restrictions by DFT methods, using the BP86 functional and the numerical basis set DN*, which includes *d*-type polarization functions for all non-hydrogen atoms. The gradient correction was included in a perturbative manner only after convergence on a local potential was achieved (pBP method). The geometry of the minima and saddle-points of the potential surface were checked with frequency calculations. For the calculation of the geometry of “real” molecules containing *iso*-propyl substituents, a guess model of the molecular geometry was built starting from the results of a previous calculation on the simplified molecules, and those underwent molecular mechanics conformational analysis (MMFF, Merck Molecular Force Field), while maintaining fixed positions of the core atoms. The geometry of the five more stable conformers underwent full optimization without restraints by using the DFT method, and the lower computed energies were used in the thermochemical and activation barrier calculations.

Crystal structure of 15: A summary of the conditions for data collection is given in Table 3. A pale-yellow crystal of prismatic shape was coated with an epoxy resin and mounted on a Siemens Smart CCD diffractometer equipped with a normal focus, 2.4 kW sealed tube X-ray source (MoK_α radiation, λ=0.71073 Å) operating a 50 kV and 10 mA. Data were collected over a quadrant of reciprocal space by a combination of three sets of exposures. Each set had a different φ angle for the crystal and each exposure of 20 s; covered 0.3° in ω. The crystal to detector distance was 4.51 cm. Coverage of the unique set was over 99% complete to at least 23° in θ. Unit cell dimensions were determined by a least-squares fit of 40 reflections with *I*>20σ(*I*) and 6°<2θ<64°. The first 30 frames of data were recollected at the end of the data polarization effects. The structure was solved by direct methods and refined in the orthorhombic space group *P*2₁2₁2₁. Full-matrix least-square refinement with anisotropic thermal parameters for carbon and oxygen atoms and isotropic for hydrogen atoms was carried out by using SHELXTL minimizing *w*(*F*_o²–*F*_c²). Because oxygen atoms are the heavier atoms in the structure and the data was collected by using MoK_α radiation, the absolute structure could not be determined. Final difference synthesis showed no significant electron density.

All calculations were performed by using:^[19] SMART software for data collection; SAINT for data reduction and SHELXTL to solve and refine the structure and prepare material for publication. CCDC-620100 contains the supplementary crystallographic data for this paper. These data

Table 3. Crystal data and structure refinement for **15**.

Empirical formula	C ₁₇ H ₁₈ O ₄
F _w	286.31
T [K]	143(2)
λ [Å]	0.71073
Crystal system	orthorhombic
Space group	P2 ₁ 2 ₁ 2 ₁
Unit cell dimensions	
a [Å]	7.9188(11)
b [Å]	9.801(2)
c [Å]	19.158(3)
V [Å ³], Z	1487.0, 4
ρ _{calcd} [g cm ⁻³]	1.279
Absorption coefficient [mm ⁻¹]	0.091
F(000)	608
Crystal size [mm]	0.35 × 0.24 × 0.20
θ range for data collection [°]	2.78 to 32.31
Limiting indices	-11 h = 11, -14 = k = 3, -17 L = 27
Reflns collected	7520
Independent reflns	3965 (R _{int} = 0.0394)
Refinement method	full-matrix least-squares on F ²
Data/restraints/parameters	3965/0/262
Gof on F ²	1.020
Final R indices [I > 2σ(I)]	R ₁ = 0.0394, wR ₂ = 0.0956
R indices (all data)	R ₁ = 0.0440, wR ₂ = 0.0988
Absolute structure parameter	0.5(8)
Largest diff. peak and hole [eÅ ⁻³]	0.194 and -0.218

can be obtained free of charge from the Cambridge Crystallographic Data Centre via www.ccdc.cam.ac.uk/data_request/cif.

Acknowledgements

Financial support from the DGI (Project PPQ2003-000975) and Junta de Andalucía is gratefully acknowledged. C.M.M. thanks the Dirección General de Enseñanza Superior for a PFPI studentship and I.M. acknowledges a research fellowship from the Consejo Superior de Investigaciones científicas (I3P program).

- [1] a) I. Paterson in *Comprehensive Organic Síntesis, Vol 2* (Eds.: B. M. Trost, I. Fleming, C. H. Heathcock), Pergamon, Oxford, **1991**, pp. 301–319; b) C. Palomo, M. Oiarbide, J. M. García, *Chem. Soc. Rev.* **2004**, *33*, 65; c) J. Montgomery, *Acc. Chem. Res.* **2000**, *33*, 467; d) S. Kobayashi, S. Saito, M. Ueno, Y. Yamashita, *Chem. Commun.* **2003**, *14*, 2016.
- [2] a) G. M. Mahandru, A. R. L. Skauge, S. K. Chowdhury, K. K. D. Amarasinghe, M. J. Heeg, J. Montgomery, *J. Am. Chem. Soc.* **2003**, *125*, 13481; b) J. Montgomery, *Acc. Chem. Res.* **2000**, *33*, 467; c) M. Sodeoka, Y. Hamashima, *Pure Appl. Chem.* **2006**, *78*, 197.
- [3] a) D. Cuperly, J. Petriguet, C. Crévisy, René Grée, *Chem. Eur. J.* **2006**, *12*, 3621; b) S. I. Kiyooka, S. Hosokawa, S. Tukasa, *Tetrahedron Lett.* **2006**, *47*, 3959; c) Y. Hamashima, N. Sasamoto, D. Hotta, H. Somei, N. Umabayashi, M. Sodeoka, *Angew. Chem.* **2005**, *117*, 1549; *Angew. Chem. Int. Ed.* **2005**, *44*, 1525; d) A. E. Taggi, A. M. Hafez, T. Lectka, *Acc. Chem. Res.* **2003**, *36*, 1; e) T. Satoh, M. Kawamura, M. Miura, M. Nomura, *Angew. Chem.* **1997**, *109*, 1820; *Angew. Chem. Int. Ed. Engl.* **1997**, *36*, 1740; f) A. Fuji, E. Hagiwara, M. Sodeoka, *J. Am. Chem. Soc.* **1999**, *121*, 5450; g) O. Fujimura, *J. Am. Chem. Soc.* **1998**, *120*, 10032.
- [4] a) D. A. Culkin, J. F. Hartwig, *Organometallics* **2004**, *23*, 3398; b) X. Liu, J. F. Hartwig, *J. Am. Chem. Soc.* **2004**, *126*, 5182; c) M. C. Willis, D. Taylor, A. T. Gillmore, *Org. Lett.* **2004**, *6*, 4755; d) T. Hamada, A. Chieffi, J. Ahman, S. L. Buchwald, *J. Am. Chem. Soc.* **2002**, *124*, 1261; e) J. Ahman, J. P. Wolfe, M. V. Troutman, M. Palucki, S. L. Buchwald, *J. Am. Chem. Soc.* **1998**, *120*, 1918; f) G. Lu, J. L. Portscher, H. C. Malinakova, *Organometallics* **2005**, *24*, 945.
- [5] a) Y. Hamashima, D. Hotta, N. Umabayashi, Y. Tsuchiya, T. Suzuki, M. Sodeoka, *Adv. Synth. Catal.* **2005**, *347*, 1576; b) Y. Hamashima, D. Hotta, M. Sodeoka, *J. Am. Chem. Soc.* **2002**, *124*, 11240; c) M. Watanabe, A. Ikagawa, H. Wang, K. Murata, T. Ikariya, *J. Am. Chem. Soc.* **2004**, *126*, 11148; d) M. Watanabe, K. Murata, T. Ikariya, *J. Am. Chem. Soc.* **2003**, *125*, 7508.
- [6] *Comprehensi ve Organic Síntesis, Vol 4* (Eds.: B. M. Trost, I. Fleming, M. F. Sammelhack), Pergamon, Oxford, **1991**.
- [7] a) G. A. Slough, R. G. Bergman, C. H. Heathcock, *J. Am. Chem. Soc.* **1989**, *111*, 938; b) J. F. Hartwig, R. A. Andersen, R. G. Bergman, *J. Am. Chem. Soc.* **1990**, *112*, 5670; c) L. F. Hartwig, R. G. Bergman, R. A. Andersen, *Organometallics* **1991**, *10*, 3344; d) J. F. Hartwig, R. G. Bergman, R. A. Andersen, *Organometallics* **1991**, *10*, 3326; e) J. G. Stack, J. J. Doney, R. G. Bergman, C. H. Heathcock, *Organometallics* **1990**, *9*, 453; f) R. R. Burkhardt, R. G. Bergman, C. H. Heathcock, *Organometallics* **1990**, *9*, 30.
- [8] a) J. Cámpora, C. M. Maya, P. Palma, E. Carmona, C. Graiff, A. Tiripicchio, *Chem. Commun.* **2003**, 1742; b) P. Braunstein, *Chem. Rev.* **2006**, *106*, 134; c) P. Braunstein, T. M. Gomes-Carneiro, D. Matt, D. Grandjean, *Organometallics* **1989**, *8*, 1737.
- [9] E. R. Burkhardt, R. G. Bergman, C. H. Heathcock, *Organometallics* **1990**, *9*, 30.
- [10] a) J. Cámpora, C. M. Maya, P. Palma, E. Carmona, E. Gutiérrez-Puebla, C. Ruiz, *J. Am. Chem. Soc.* **2003**, *125*, 1482; b) J. Cámpora, C. M. Maya, P. Palma, E. Carmona, E. Gutiérrez, C. Ruiz, C. Graiff, A. Tiripicchio, *Chem. Eur. J.* **2005**, *11*, 6889; c) J. Cámpora, I. Matas, C. M. Maya, P. Palma, E. Álvarez, *Organometallics* **2006**, *25*, 3124.
- [11] All the stereochemical indications in the schemes refer consistently to one component of the racemic diastereomeric pairs formed in the reactions.
- [12] a) J. Cámpora, P. Palma, D. del Río, E. Álvarez, *Organometallics* **2004**, *23*, 1652; b) J. Cámpora, I. Matas, P. Palma, C. Graiff, A. Tiripicchio, *Organometallics* **2005**, *24*, 2827.
- [13] a) J. Cámpora, P. Palma, D. del Río, M. M. Conejo, E. Álvarez, *Organometallics* **2004**, *23*, 5653; b) J. Cámpora, J. A. López, C. M. Maya, P. Palma, E. Carmona, P. Valerga, *J. Organomet. Chem.* **2002**, *644*, 331.
- [14] L. Pauling, *The Nature of the Chemical Bond*, Cornell University Press, **1960**.
- [15] a) F. A. Carey, R. J. Sundberg, *Advanced Organic Chemistry*, 3rd ed. Plenum Press, New York, **1990**, Part A, pp. 147–149; b) E. Juaristi, G. Cuevas, *The Anomeric Effect*, CRC Press: Boca Raton, Florida, **2000**.
- [16] a) A. R. Kathrizki, A. F. Pozarskii, *Handbook of Heterocyclic Chemistry*, 2nd ed. Pergamon, Oxford, **2000**, p. 247; b) M. B. Smith, J. March, *Advanced Organic Chemistry. Reactivity, Mechanisms and Structure*. 5th ed., Wiley, New York, **2001**; c) T. W. Greene, P. G. M. Wuts, *Protective Groups in Organic Synthesis*, 2nd ed., Wiley, New York, **1991**.
- [17] W. Carruthers, *Cycloaddition Reactions in Organic Synthesis*, Pergamon Press, Oxford, **1990**, p. 108.
- [18] Mac Spartan Pro, Vers. 1.0.4. Wavefunction, 18401 Von Karman, Suite 370, Irvine, California 92612.
- [19] Siemens Energy and Automation, Analytical Instrumentation, **1996**.

Received: September 20, 2006
Published online: January 26, 2007